Unraveling Anthropocene Paleoenvironmental Conditions Combining Sediment and Foraminiferal Data: Proof-of-Concept in the Sepetiba Bay (SE, Brazil)

Layla Cristine Da Silva, Maria Virgínia Alves Martins, Rubens Figueira, Fabrizio Frontalini, Egberto Pereira, Thaise Senez-Mello, Wellen Fernanda Louzada Castelo, Murilo Barros Saibro, Fabio Francescangeli, Silvia Helena Mello E Sousa, et al.

frontiers in Ecology and Evolution

ORIGINAL RESEARCH
published: 28 March 2022
doi: 10.3389/fevo.2022.852439

Unraveling Anthropocene Paleoenvironmental Conditions Combining Sediment and Foraminiferal Data: Proof-of-Concept in the Sepetiba Bay (SE, Brazil)

Layla Cristine da Silva[1†], Maria Virgínia Alves Martins[1,2†], Rubens Figueira[3], Fabrizio Frontalini[4†], Egberto Pereira[1†], Thaise M. Senez-Mello[5†], Wellen Fernanda Louzada Castelo[1†], Murilo Barros Saibro[1], Fabio Francescangeli[6†], Silvia Helena Mello e Sousa[3], Sérgio Bergamaschi[1], Luzia Antonioli[1†], Vincent M. P. Bouchet[7†], Denise Terroso[2] and Fernando Rocha[2]*

[1] Universidade do Estado do Rio de Janeiro, UERJ, Faculdade de Geologia, Rio de Janeiro, Brazil, [2] Universidade de Aveiro, GeoBioTec, Departamento de Geociências, Aveiro, Portugal, [3] Instituto Oceanográfico, Universidade de São Paulo (IOUSP), São Paulo, Brazil, [4] Department of Pure and Applied Sciences, Università degli Studi di Urbino "Carlo Bo", Urbino, Italy, [5] Marine Geology Lab–LAGEMAR, Federal Fluminense University (UFF), Rio de Janeiro, Brazil, [6] Department of Geosciences, University of Fribourg, Fribourg, Switzerland, [7] Univ. Lille, CNRS, Univ. Littoral Côte d'Opale, IRD, UMR 8187, LOG, Laboratoire d'Océanologie et de Géosciences, Station Marine de Wimereux, Lille, France

The Sepetiba Bay (SB), located in the state of Rio de Janeiro (SE Brazil), is a transitional ecosystem highly anthropized. Because of its great environmental, economic, and social importance, the SB has been the target of several studies to investigate the sources of pollution and their environmental impact. However, studies on the response of foraminifera to pollution are rare. This study applies for the first time in the SB the Ecological Quality Ratio (EQR) based on the biotic index exp(H'_{bc}), related to foraminiferal diversity, coupled with granulometric, mineralogical, and geochemical data and a robust age model (based on ^{210}Pb and ^{137}Cs activity). This study aims to evaluate the paleo-ecological quality status (PaleoEcoQS) along core SP5, collected in the inner central region of the SB. In the sedimentary record of the first half of the 20th century, no foraminifera were found, and the moderate enrichment in lithogenic elements was probably related not only to weathering and erosion of rocks but also to mining activities in the region. From the second half of the 20th century, the study area was under higher marine influence. Progressive siltation took place because of anthropogenic interventions in river courses, eutrophication, and metal pollution. Weak hydrodynamic conditions favored the accumulation of fine-grained sediments and organic matters. In the same period, low diversified benthic foraminiferal assemblages, including mainly opportunist species, were developed. Paleo-ecological conditions inferred by the biotic index exp(H'_{bc}) were poor around 1970 and worsened after the metal spill released by Companhia Ingá Mercantil (a zinc ore processing plant). After that, progressively recovery has led to good ecological conditions in 2015. This study shows how benthic foraminiferal methods could represent a very useful tool to track changes in the evaluation of PaleoEcoQS.

Keywords: environmental quality assessment, transitional water, sediment, tropical, multiproxy approach, meiofauna

OPEN ACCESS

Edited by:
Gael Le Roux, UMR 5245 Laboratoire Ecologie Fonctionnelle et Environnement (ECOLAB), France

Reviewed by:
Joel Knoery, Institut Français de Recherche pour l'Exploitation de la Mer (IFREMER), France
Veronica Rossi, University of Bologna, Italy
Thomas Gloaguen, Federal University of the Recôncavo of Bahia, Brazil

***Correspondence:**
Maria Virgínia Alves Martins
virginia.martins@ua.pt

†ORCID:
Layla Cristine da Silva
orcid.org/0000-0002-0747-5987
Maria Virgínia Alves Martins
orcid.org/0000-0001-8348-8862
Fabrizio Frontalini
orcid.org/0000-0002-0425-9306
Egberto Pereira
orcid.org/0000-0002-9705-2784
Thaise M. Senez-Mello
orcid.org/0000-0002-2246-7117
Wellen Fernanda Louzada Castelo
orcid.org/0000-0001-7974-1546
Fabio Francescangeli
orcid.org/0000-0002-8309-3315
Luzia Antonioli
orcid.org/0000-0002-7846-6324
Vincent M. P. Bouchet
orcid.org/0000-0001-5458-1638

Specialty section:
This article was submitted to Paleoecology, a section of the journal Frontiers in Ecology and Evolution

Received: *11 January 2022*
Accepted: *25 February 2022*
Published: *28 March 2022*

INTRODUCTION

Over the last decades, degradation of coastal and transitional waters has attracted the attention of the international scientific community (Elliott and Quintino, 2007; Blanchet et al., 2008; Bouchet et al., 2018a,b, 2020). Many coastal areas in the world are nowadays facing pollution problems, for instance, the Stege tidal marsh in the United States (Hwang et al., 2006), the Aveiro lagoon in Portugal (Martins et al., 2015), the Odiel River in Spain (Santos Bermejo et al., 2003), the Er-Rbia Estuary in Morocco (Asfers et al., 2017), the Izmit Bay in Turkey (Pekey, 2006), the Caspian Sea Coast (Abadi et al., 2019), coastal areas of Black Sea, the Marmara Sea and the Aegean Sea (Balkıs et al., 2007), the Bohai Bay in China (Gao and Chen, 2012), and the Cochin estuary in India (Salas et al., 2017). In the last century, several Brazilian estuarine ecosystems were affected by pollution due to increase in human activities, for instance, in mangrove zones of the Amazon coast (NE Brazil; Jesus et al., 2021), the Ipojuca River Estuary (Pernanbuco, Silva et al., 2019), the Green Coast Region (GCR), the state of Rio de Janeiro (SE Brazil; Souza et al., 2021), the Santos Estuary (São Paulo State, SE Brazil; Jesus et al., 2020), and the Patos Lagoon (SE Brazil; Moreira, 2012). Pollution in these environments was caused by mining, installation of industrial complexes, burning of fossil fuel, emission of domestic liquid effluents, and port activities. Worsening of environmental quality was extremely intense in the Sepetiba Bay (SB) located in the GCR (SE Brazil) (Barcellos et al., 1997; Copeland et al., 2003; Freret-Meurer et al., 2010; Ribeiro et al., 2013; Ferreira and Moreira, 2015; Araújo et al., 2017a,b; Alves Martins et al., 2019a; Díaz Morales et al., 2019; Castelo et al., 2021a,b; Quaresma et al., 2021; Souza et al., 2021). Since 1950, with expansion of industrial, municipal, agricultural, and harbor activities, a large amount of contaminants has been discharged into this bay, resulting in overall degradation of this ecosystem (Wasserman et al., 2001; Castelo et al., 2021a,b). The SB and pollution effects on the biota have been, therefore, the target of several studies (e.g., Amado-Filho et al., 1999; Araújo et al., 2002; Lacerda and Molisani, 2006; Carneiro et al., 2013). High concentrations of heavy metals were responsible for the 60% reduction in fish population (Kato and Quintela, 2012). Metal contamination is, in fact, one of the main environmental legacies generated by the industrial and urban development of the region (Pellegatti et al., 2001; Rodrigues et al., 2020; Souza et al., 2021). The industrial complex and Companhia Ingá Mercantil (CIA Ingá; a zinc ore processing plant) are considered as the main source of heavy metal discharge into the SB (Lacerda et al., 1987; Molisani et al., 2004; Paraquetti et al., 2004).

To further complement the assessment of geochemical features of the environment, it is necessary to consider how benthic communities are affected by the worsening of ecological conditions. For this purpose, benthic foraminifera have been increasingly used as a witness of environmental degradation (e.g., Alve, 1995; Bouchet et al., 2018a; Francescangeli et al., 2020). Thus, foraminiferal-based biotic indices have been developed to quantitatively evaluate environmental quality in a wide variety of marine and brackish ecosystems (e.g., Barras et al., 2014; Alve et al., 2016; Bouchet et al., 2021). Foraminifera are single-celled organisms with a short life and reproductive cycle. Because of their rapid response to environmental stimuli (e.g., increasing of organic matters, metal pollution), they reflect the environmental conditions in the area in which they live (e.g., Murray, 2006; Martins et al., 2015). Furthermore, because of their fossilizable tests (i.e., shell), they are excellent paleoenvironmental indicators in the sedimentary record (e.g., Francescangeli et al., 2018). In polluted coastal areas, they were successfully used to distinguish pre-impacted (reference conditions) from impacted ones (Francescangeli et al., 2016; Hess et al., 2020; Jesus et al., 2020). Several studies have addressed present and past distributions of benthic foraminifera and their response to pollution in the SB (Amado-Filho et al., 1999; Barbosa, 2005; Martins et al., 2019; Castelo et al., 2021a). However, there is still lack of knowledge of how foraminiferal faunas respond to the recent evolution of the SB.

In this context, this study intends to reconstruct paleo-ecological quality status (PalaeoEcoQS) using for the first time in SB a foraminiferal-based biotic index ($\exp(H'_{bc})$). This index was recently applied in the Santos estuary (Jesus et al., 2021), and there is a need to test its functionality in other coastal Brazilian ecosystems. This index is related to benthic foraminiferal diversity by assessing the deviation from reference conditions (i.e., pre-impacted conditions). Over the last ≈150 years, paleo-community changes have been coupled with textural, mineralogical, and geochemical data to better trace the paleoenvironmental evolution of the SB.

STUDY AREA

The SB is a coastal body in the southern part of the state of Rio de Janeiro (SE Brazil) (**Figure 1**). Its east-west axis is 43 km long, and its north-south axis is about 17 km wide (Paraquetti et al., 2004). The SB covers the region of Sepetiba, Itaguaí, and Mangaratiba. It is a semi-confined coastal system, limited to the north by the continent, to the east by the Guaratiba coastal plain, to the south by the Marambaia Barrier Island, and to the west by a system of islands with migmatitic rocks. This setting influences internal hydrodynamic conditions, isolating the inner bay and protecting this environment from the direct action of marine processes (Paraquetti et al., 2004). It is connected to the ocean through two channels (with widths of ≈2 km) located in opposite portions of this system. The first channel, in the western portion of the bay, is natural, whereas the second one, in the eastern sector of the bay, is artificial that connects the Barra de Guaratiba region to the ocean.

The region is characterized by a warm and humid subtropical climate (Kottek et al., 2006; Peel et al., 2007), with an average annual rainfall varying between 1,400 and 2,500 mm (Lacerda et al., 2001; Paraquetti et al., 2004). Highest precipitation rates are recorded during spring, while autumn and winter have a drier climate (Villena et al., 2012). Its hydrographic basin with an area of 2,165 km^2 consists of nine rivers, including Guandu, Guandu-Mirim, and Guarda rivers (Dourado et al., 2012). These rivers contribute to annual freshwater flow of approximately 7.6 million m^3 (Lacerda et al., 2001). The Guandu River is responsible for

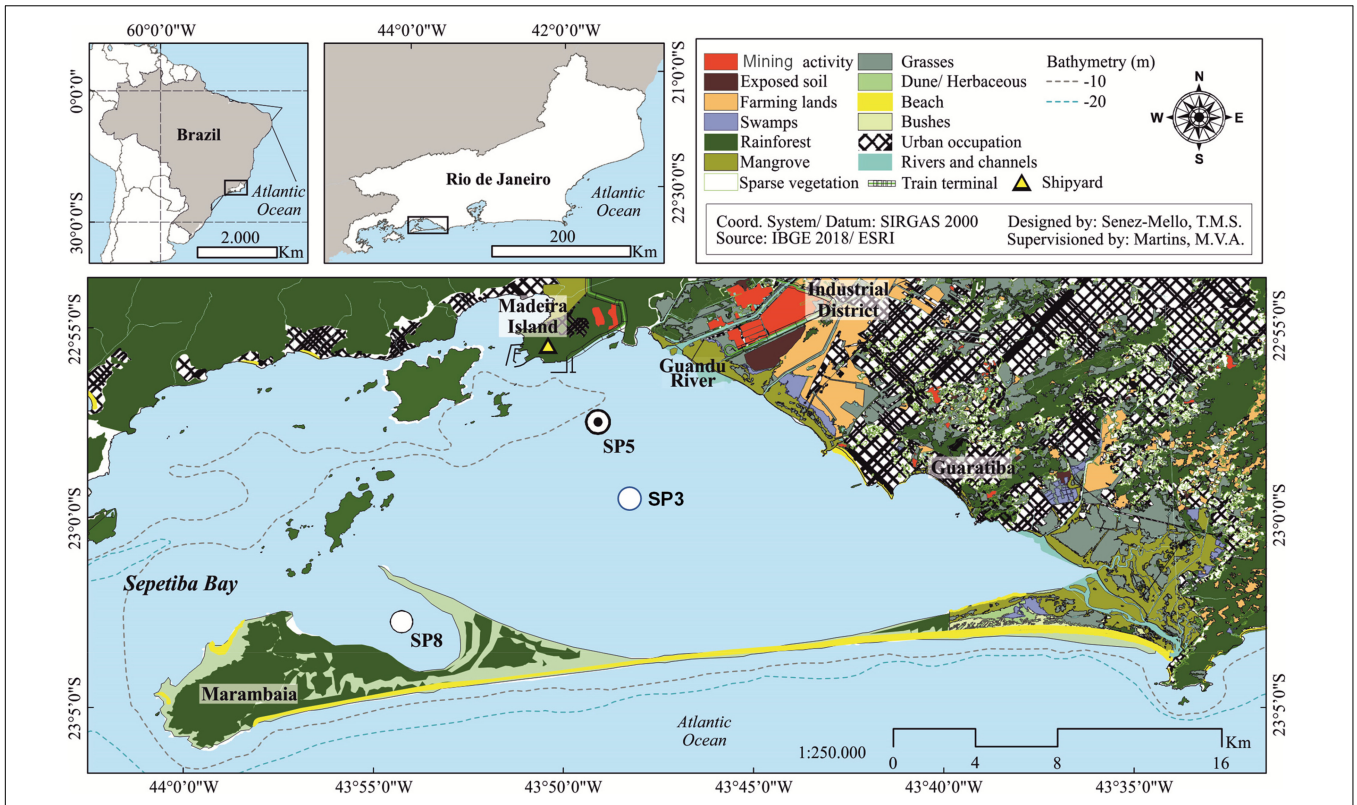

FIGURE 1 | Study area and location of core SP5, as well as core SP8 used for the calculation of Ecological Quality Ratio, and core SP3.

providing much of the drinking water to the metropolitan region of Rio de Janeiro (Lacerda et al., 2004). SB hydrodynamics is controlled by fluvial contribution and by the action of winds and tides. The tides are semidiurnal (Kjerfve et al., 2021) and their amplitude is <2 m. Water renewal time in the inner region of the SB is about 100 h (Paraquetti et al., 2004). Average wind speeds from the north, northeast, and east are predominant, ranging from 1.6 to 5.5 m/s and occasionally reaching up to 8.8 m^{-1}; winds from the east and southwest (blow ≈10% of the time) sometimes exceed 11 m s^{-1} during the passage of cold fronts (Kjerfve et al., 2021). The velocity of currents varies between < 20 and 40 cm^{-1} throughout the bay, but higher velocities were recorded at the bay entrance (50 to 75 cm $^{-1}$) (Molisani et al., 2004). The average water temperature and dissolved oxygen concentration in the water column are 25°C and 8 mg L^{-1}, respectively. The average salinity value is about 32, but it reduces near the mouths of main rivers (Cunha et al., 2006).

The SB encompasses two distinct geomorphological domains: mountainous and lowlands. The former is characterized by mountains and escarpments of the Serra do Mar and by the coastal massifs of Pedra Branca, Mendanha, and Marambaia Island. The domain of lowlands, on the other hand, is characterized by fluvio-marine plains that are intercepted by several rivers flowing into the SB (SEMADS, 2001).

The lithology of the region is composed of Proterozoic rocks with an NE-SW structural trend, and lowland areas are covered with Neogene sediments (Roncarati and Carelli, 2012; Heilbron et al., 2020). Sediments that make up the substrate of the bay vary from sand to mud. Nowadays, muddy sediments cover about 70% of the bottom, being the predominant granulometry in the inner area of the bay (Borges and Nittrouer, 2016a,b). Sandy sediments predominate next to the São Francisco Canal mouth, in the outermost areas of SB and close to Marambaia Barrier Island (Villena et al., 2012; Borges and Nittrouer, 2016a,b). Sedimentation in the SB is controlled by a mixture of sources: fluvial, marine, and autochthonous (for instance, trough biogenic and diagenetic contributions). Sediments of fluvial origin are predominant in the inner eastern region, while marine contribution to coastal deposits occurs mainly in the western part (Barcellos et al., 1997). Aluminosilicates, indicative of continental influence, are important constituents of bottom sediments of the SB and are, in general, related to high concentrations in trace metals (Rodrigues et al., 2020; Souza et al., 2021).

MATERIALS AND METHODS

Core Collection and Processing

This study is based on the analysis of core SP5 (140-cm long), collected in the western portion of the SB (UTM: 0621164/7460621; 23K, WGS84), near Madeira island (**Figure 1**). Core SP5 was collected by divers using the percussion probing method. After collection, this core was sealed and transferred

to the Micropaleontology Laboratory of the Universidade do Estado do Rio de Janeiro (UERJ), Faculty of Geology (LabMicro/UERJ), where it was frozen. After that, the whole core was defrosted, opened, and described. Since the core had no sedimentological discontinuities, it was continuously sampled at 2- to 3-cm intervals. Sixty sediment samples were obtained and devoted to granulometric, geochemical, mineralogical, and benthic foraminiferal analyses. This core was dated with ^{210}Pb and ^{137}Cs.

Granulometry and Mineralogy

For particle size analysis, about 10 g of total sediment per sample was used (although small in amount, it should be representative of the sample given its homogeneity). The sediment was washed through a 63-μm mesh sieve to separate the <63 μm and >63 μm fractions. Both fractions were collected and oven-dried at low temperature (60°C). After drying, the sediment fractions were weighed and stored. Samples from sedimentary fraction >63 μm were separated by a set of sieves with different mesh sizes (i.e., 63, 125, 250, 500, and 1,000 μm). The sediment contained in each sieve was weighed to determine the percentage of each particle size. Textural classification of these sediments was based on the classifications of Folk and Ward (1957).

Sedimentary fraction <63 μm (silt-clay fraction) was used in the mineralogical analysis. It was separated with distilled water from the coarser sediment fractions. For the mineralogical analysis by X-ray diffraction (XRD) technique, about 3 g of sediment was dried in an oven at low temperature and disaggregated in an agate mortar. XRD measurements were performed using the Philips PW1130/90 and X'Pert PW3040/60 devices at the Aveiro University (Portugal), which used Cu Kα radiation. Scans were performed between 2 and 60° 2θ (in unoriented powder assemblies). The identification and semi-quantification of minerals followed the methodology described by Martins et al. (2007).

Geochemical Analyses

Calcium Carbonate, Total Organic Carbon, Total Sulfur, and Insoluble Residue

The samples (ca. 5 g) were powdered in an agate mortar and sieved with a 125-μm mesh sieve (to remove coarser particles). The samples were then decarbonated by acidification with 50% HCl for a period of approximately 12 h, washed with distilled water, and dried in an oven at low temperature (60°C). Insoluble residue (IR) and carbonate content ($CaCO_3$) were determined. After the decarbonation process, total organic carbon (TOC) and total sulfur (S) were analyzed with the LECO SC-632 equipment. These analyses were carried out in the Laboratory of Chemical Stratigraphy and Organic Geochemistry (LGQM) of the Faculty of Geology of UERJ. C/S ratio, widely used as a redox indicator of the environment and sediment (Lyons and Berner, 1992; Algeo and Liu, 2020; Liu et al., 2021), was determined from the TOC (in %) and S (in %) values.

Elemental Geochemistry

About 5 g of sediment from each dry sample was powdered in an agate mortar and sieved with a 63-μm mesh sieve. Elemental geochemical analysis was performed after total digestion with four acids (HNO_3, $HClO_4$, HF, and HCl) by inductively coupled plasma-mass spectrometry (ICP-MS) at the Bureau Veritas LTDA laboratory (certified under ISO/IEC 17025), Vancouver, Canada (in sediment fraction <63 μm). The quality of data was assessed using the analytical results of certified standard materials (STD OREAS45E and STD OREAS25A-4A), blanks, and random duplicate samples. The results were within the 95% confidence limit of recommended values given for the certified materials. Uncertainties of the results were <7%. Concentrations of 41 chemical elements were determined.

The enrichment of chemical elements whose concentrations reached values above the world shale (Turekian and Wedepohl, 1961) and local baseline values (estimated by Pinto et al., 2019) was estimated in core SP5 for Al, As, Cd, Ce, Fe, Hf, Mn, Mo, Nb, P, Pb, S, Sn, Th, U, W, Zn, and Zr with enrichment factor (EF). EF values were estimated according to the procedure suggested by Buat-Menard and Chesselet (1979) using the formula:

$$EF = \frac{\left(\frac{Cx}{Cn}\right)\ Sample}{\left(\frac{Cx}{Cn}\right)\ Baseline}$$

where Cx corresponds to the concentration of the element whose enrichment is to be determined (x), and Cn is the concentration of the normalizing element (n) in the sample. The baseline values estimated by Pinto et al. (2019; **Table 1**) were used. For elements whose background values are not available in Pinto et al. (2019), mean elemental concentrations of the worldwide shale of Turekian and Wedepohl (1961; **Table 1**) were considered. Scandium (Sc) was used as a normalizer, because it is a lithogenic chemical element, and in the SB, it has higher correlation with fine grained sediments than Al (Castelo et al., 2021a,b). Geoaccumulation Index (Igeo), which is widely applied to assess environmental pollution, was determined (for Al, As, Cd, Ce, Fe, Hf, Mn, Mo, Nb, P, Pb, S, Sn, Th, U, W, Zn, and Zr) in accordance with Müller (1986):

$$\text{Igeo} = \log_2\left[\frac{Cn}{Bn\ \text{x}\ 1.5}\right]$$

where Cn is the metal concentration (n) in the sample and Bn the respective baseline concentration.

The ecological risk index (RI) of every potentially toxic metal with EF value > 2 (As, Cd, Pb, Sn, and Zn) (Håkanson, 1980) was determined with the equation:

$$\text{RI} = T_{rf} \times \text{CF}$$

where T_{rf} is a metal's toxic response factor. The following values of T_{rf} were considered: Zn and Sn = 1; Pb = 5; As = 10, and Cd = 30 (Håkanson, 1980; Swarnalatha et al., 2013; Zheng et al., 2020). The value of T_{rf}: for Sn was considered 1, since it was not determined in the literature as far as we know.

Concentration factor (CF) estimates the increase of a chemical element (Cn) in relation to its baseline concentration (Bn) in the sediments (Håkanson, 1980) and was calculated as:

$$CF = \frac{C_n}{B_n}$$

Potential ecological risk index (PERI) was calculated as the sum of individual potential hazards (RI) in accordance with Swarnalatha et al. (2013): PERI = ΣRI = $\Sigma(T_{rf}$ x CF). The classification of referred geochemical indices is shown in **Table 2**.

Stable Isotopes ($\delta^{13}C$ and $\delta^{15}N$) and N Concentration in Organic Matter

About 3 g of dry sediment was acidified in order to eliminate carbonates and determine the values of $\delta^{13}C$ in organic matter (hereafter referred to only as $\delta^{13}C$). For this analysis, the sediment was powered in an agate mortar and sieved through a 63-μm mesh sieve. The samples were stored in tin capsules and transferred to a FLASH EA 1112 SERIES instrument (responsible for elemental analysis) and DELTA V ADVANTAGE (spectrophotometer) from Thermo Fisher Scientific. These analyses were carried out at the Laboratory of Chemical Stratigraphy and Organic Geochemistry (LGQM) of the Faculty of Geology of UERJ. The standard deviation of the $\delta^{13}C$ data was ±0.043‰.

Total (non-acidified) samples were used for the analysis of total nitrogen (TN) and to determine the $\delta^{15}N$ values. Between 6 and 8 mg of dry sediments were placed in tin capsules and then analyzed with the Advantage MS Thermo Scientific Delta V (EA-IRMS) equipment coupled to a Costech elemental analyzer from the Oceanographic Institute, University of São Paulo (Brazil).

TABLE 1 | Baseline values: (A) Shale (according to Turekian and Wedepohl, 1961); (B) Local to Sepetiba Bay (according to Pinto et al., 2019).

Elemental Concentrations		A.	B.
		Baseline Values	*Baseline* Values
Ag	mg kg^{-1}	0.07	0.7
Al	%	8.0	8.3
As	mg kg^{-1}	13	16.6
Ba	mg kg^{-1}	580	160.3
Be	mg kg^{-1}	3	2.3
Bi	mg kg^{-1}	….	….
Ca	%	2.2	1.0
Cd	mg kg^{-1}	0.3	0.5
Ce	mg kg^{-1}	59	….
Co	mg kg^{-1}	19	8.8
Cr	mg kg^{-1}	90	68.1
Cu	mg kg^{-1}	45	14.3
Fe	mg kg^{-1}	4.7	4.9
Hf	mg kg^{-1}	2.8	….
K	%	2.7	1.8
La	mg kg^{-1}	92	40.7
Li	mg kg^{-1}	66	….
Mg	%	1.5	1.4
Mn	mg kg^{-1}	850	431.4
Mo	mg kg^{-1}	2.6	3.8
Na	%	9.6	1.1
Nb	mg kg^{-1}	24	19.3
Ni	mg kg^{-1}	68	23.3
P	%	0.07	0.06
Pb	mg kg^{-1}	20	24.2
Rb	mg kg^{-1}	140	….
S	%	0.24	1.8
Sb	mg kg^{-1}	1.5	….
Sc	mg kg^{-1}	13	11.8
Sn	mg kg^{-1}	6.0	3.7
Rb	mg kg^{-1}	140	….
Re	mg kg^{-1}	6	3.7
Sr	mg kg^{-1}	300	121.3
Ta	mg kg^{-1}	0.8	….
Th	mg kg^{-1}	12	14.6
Ti	%	0.46	0.52
U	mg kg^{-1}	3.7	….
V	mg kg^{-1}	130	87.3
W	mg kg^{-1}	1.8	….
Y	mg kg^{-1}	26	16.9
Zn	mg kg^{-1}	95	82.3
Zr	mg kg^{-1}	160	80.1

Dating With Pb^{210} and Cs^{137}

For the ^{210}Pb and ^{137}Cs analyses, about 15 g of dry sediment was used. Twenty samples were disaggregated in an agate mortar and analyzed in an EG&G ORTEC (Hyperpure Ge, model GMX25190P) gamma spectrometer at LaQIMar (Laboratory of Marine Inorganic Chemistry, University of São Paulo, Brazil). Ages were based on a constant sedimentation model in accordance with Figueira et al. (2007) and Ferreira et al. (2014).

Benthic Foraminifera

Samples of 10 ml of sediment were used to assess foraminiferal assemblages. The sediment samples were washed with distilled water in a 63-μm sieve. Fractions <63 μm and >63 μm were stored in beakers and oven-dried at low temperature (<60°C). Foraminifera from fraction >63 were picked from a volume of 10 ml and placed in foraminiferal slides with the aid of a mink hair brush and a Zeiss microscope, model Stemi SV11, with a maximum magnification of 200×.

For species identification, the Ellis and Messina catalog (Ellis and Messina, 1940-2015) was consulted, as well as specific references, such as Loeblich and Tappan (1987), for the identification of genera, and Boltovskoy et al. (1980), Debenay et al. (2001), Martins and Gomes (2004), and Alves Martins et al. (2019a) for identification at specific level. The online catalog available at WoRMS (World Register of Marine Species; Hayward et al., 2020) was also used to update the name of species.

Foraminiferal density (FD) was calculated as the number of tests found in 10 ml of sediment (n°/10 ml). Species richness (SR; number of species present in a sample) was calculated for all samples with foraminifera. The exp(H'_{bc}) and evenness (J') indexes were estimated only for samples with a number ≥100 specimens/10 ml. According to Fatela and Taborda (2002), this is the smallest number of individuals that will allow us to characterize foraminiferal assemblage with reliability. Thus, only these parameters were determined in samples between 0 and 32 cm of core SP5. SR and evenness (J') index were determined with the Primer 06 software.

The biotic index exp(H'_{bc}), based on foraminiferal diversity, was evaluated according to Bouchet et al. (2012). It was used to evaluate paleo-ecological quality status (PaleoEcoQS) [for details, see Bouchet et al. (2012) and Francescangeli et al. (2016)].

TABLE 2 | Reference for the classification of enrichment factor (EF; Sutherland, 2000), geoaccumulation index (Igeo; Müller, 1986), ecological risk index (RI; Protano et al., 2014), individual by sample, and potential ecological risk index (PERI) as a whole per sample (Håkanson, 1980; Swarnalatha et al., 2013).

EF Levels	EF Classification	Igeo Levels	Igeo Classification	PERI Levels	PERI Effects
E < 2	Null or minimal contamination	**<0**	Unpolluted	**<150**	Low ecological risk
2 < EF < 5	Moderate enrichment	**0–1**	Unpolluted to moderately polluted	**150–300**	Moderate ecological risk
5 < EF < 20	Significant enrichment	**1–2**	Moderately polluted	**300–600**	Considerable ecological risk
20 < EF < 40	Very high enrichment, indicating high level of contamination	**2–3**	Moderately to strongly polluted	**>600**	Very high ecological risk
EF>40	Extremely high enrichment, indicating extreme contamination	**3–4**	Strongly polluted	.....	.....
.....	.....	**4–5**	Strongly to extremely polluted	.....	.....
.....	.....	**>5**	Extremely polluted	.....	.....

The EF, Igeo and PERI ranges are in bold.

Ecological Quality Ratio (EQR) was further calculated to make a more accurate assessment of PaleoEcoQS. EQR is the ratio between the value of a biological metric [diversity in our case, i.e., $\exp(H'_{bc})$] and the expected value under reference conditions. Benthic foraminiferal assemblages from the SB, found in core SP8 (Castelo et al., 2021b; **Figure 1**), were used to infer pre-impacted reference conditions. Core SP8 records natural and anthropic forcing in the last ∼9.5 ka BP. The application of Foram Stress Index (FSI) and $\exp(H'_{bc})$ allowed us to identify sedimentary layers that characterize a system with maximum health at ≈5 ka BP during the mid-Holocene relative sea-level highstand. The $\exp(H'_{bc})$ of the assemblage associated to the maximum health of this system (recorded in core SP8 by Castelo et al., 2021b) was taken as a reference to estimate EQR. Five equal-size class boundaries were categorized as follows: 1–0.8, high; 0.8–0.6, good; 0.6–0.4, moderate; 0.4–0.2, poor; and 0.2–0, bad EcoQs. The package "entropy" (Hausser and Strimmer, 2014) in the R software (R Core Team, 2016) was used to calculate $\exp(H'_{bc})$.

In addition, *Ammonia-Elphidium* Index (AEI) was used to infer changes in oxygenation conditions of the bottom environment. Both genera are common in coastal and transitional waters; however, *Ammonia* dominates in low-oxic bottom waters and/or sediments (Duleba et al., 2018, 2019). This index was estimated with the equation $AEI = [NA/(NA + NE)] \times 100$ (Sen Gupta et al., 1996), where NA is the number of *Ammonia* specimens, and NE is the number of *Elphidium/Cribroelphidium* specimens. The AEI values range from 0 (well-oxygenated) to 100% (dysoxic-anoxic).

Statistical Treatment

For statistical analysis of the granulometry data, the Gradistat software (Blott and Pye, 2001) was used to obtain parameters such as sediment mean grain size (SMGS), mode, sorting, skewness, and kurtosis of the analyzed samples.

The relationship among mineralogical, geochemical, isotopic, and abundance of benthic foraminifera data was analyzed by Spearman correlations and principal component analysis (PCA) in Statistica v.13 (TIBCO Software Inc, 2018). Variables were categorized into layers and converted into years according to age estimations based on ^{210}Pb and ^{137}Cs (**Supplementary Table 1**).

For the PCA, variables were reduced according to the criteria: (i) element with concentration values below detection levels or sparse data (< 10 valid cases), (ii) redundancy–r > 0.9 (the variable with highest correlation with the matrix–Pearson correlation was retained), and (iii) invariance check (coefficient of variation threshold < 0.01). The data were standardized using the "ranging for variables with arbitrary zero" procedure. The goal of normalization was to change the values of numerical columns in the data set to a standard scale without distorting differences in the ranges of values (Milligan and Cooper, 1985). The analyzed components were those that exhibited eigenvalues higher than 1. Foraminiferal abundances were computed in the PCA as supplementary variables and, therefore, did not influence the other variables. The PCA plot is a representation of the correlations between active variables (environmental), supplementary variables (species) and the cases (years). Components with eigenvalues greater than 1 were retained.

In addition, a canonical correspondence analysis (CCA), which is a multivariate ordination technique, was also performed using version 7 of the PC-ORD software (McCune and Mefford, 2016), aiming to extract major gradients among biotic and abiotic variables and samples (represented by years).

RESULTS

Geochronology

Core SP5 has a light brownish gray (at the middle part) to dark gray or black color. No abrupt transitions or apparent sedimentary structures were observed. The age model of this core, based on ^{210}Pb data presented in **Supplementary Table 1**, reveals that it records the last ≈150 years, with an average accumulation rate of $\approx 0.83 \pm 0.13$ cm year^{-1}. The maximum fallout of ^{137}Cs, corresponding to 1963, was recorded at the 45-cm level.

Granulometry

Core SP5 is a sandy-mud and muddy-sand sedimentary sequence (**Supplementary Table 2**), with sediment mean grain size (SMGS) of $\approx 40 \pm 15$ μm. The percentage of the fine fraction (<63 μm) varies between 30.4 and 81.1% (with an average equal to 59.6%).

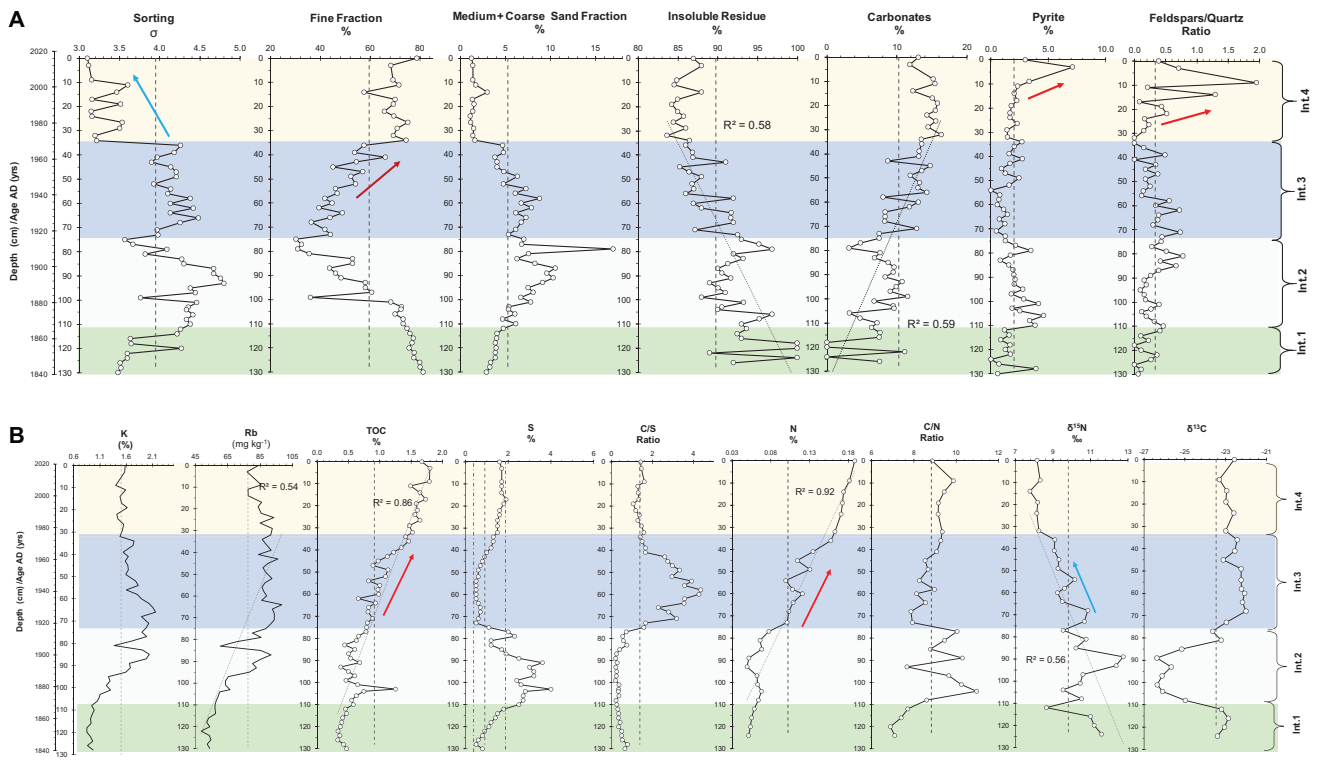

FIGURE 2 | Graphs as a function of depth and age (Anno Domini or AD) of: **(A)** sorting, percentage of fine fraction, medium and coarse sand, carbonates, and pyrite and feldspar/quartz ratio; **(B)** SMGS (in %; sediment mean grain size), TOC (in %; total organic carbon), C/S, N (in %), $\delta^{15}N$ (in ‰), and $\delta^{13}C$ in (‰). Based on the analyzed data, four intervals (Int.) are highlighted. Red and blue dashed vertical lines correspond to global baseline values for shale (Turekian and Wedepohl, 1961) and for local fine sediments (Pinto et al., 2019), respectively. The arrows highlight variables with increasing (in red) or decreasing (lower) concentration trends. The regression line for some variables and their R^2 value are also presented.

The fine fraction is predominant both at the base and at the core top, while the sand fraction increases in the middle section of the core (**Figure 2**), where SMGS reaches 74.4 μm (**Supplementary Table 2**). At the top of the core, the sediments are bimodal, while in the intermediate portion and at the base of the core, the sediments are polymodal. The sediments are predominantly composed of 3 modes, 76.5, 152.5, and 605 μm. Sorting values (σ) reveal that the sediments are generally poorly sorted in the upper and lower sections of the core and are very poorly sorted in the intermediate zone, and have coarser granulometry.

Mineralogy

The main mineralogical constituents are (**Supplementary Table 2**): phyllosilicates (48.3–87.35%, mean: 72.19 ± 7.5%), followed by quartz (7.99–31.94%, mean: 16.82 ± 4.84%), K-feldspar (0–16.45%, mean: 3.65 ± 3.26%), and plagioclase (011.39%, mean: 1.5 ± 2.51%). The accessory constituents are calcite (07.9%, mean:0.69 ± 1.49%), pyrite (0–7.13%, mean: 1.94 ± 1.21%), zeolites (0–4.84%, mean:0.27 ± 0.88%), siderite (0–4.67%, mean:0.85 ± 1.34%), anatase (0–4.39%, mean: 1.09 ± 1.41%), anhydrite (0–4.25%, mean.78 ± 1.17%), magnetite/maghemite (0–2.82%, mean:0.19 ± 0.57%), ilmenite (0–1.35%, mean:0.09 ± 0.31%), and dolomite (0–0.85%, mean:0.03 ± 0.15%). Significant changes in mineralogical composition of the sediments along the core are not observed. However, the presence of pyrite and increase of this mineral in the upper part of the core, as well as rise in feldspar/quartz ratio values should be noted. The values of this ratio also increase slightly in the middle part of the core (**Figure 2A**).

Geochemical Parameters

Total organic carbon (0.33–1.8%, mean:0.91 ± 0.45%) and N (0.049–0.188%, mean:0.104 ± 0.046%) contents tend to continuously increase from 80 cm to the upper part of the core. The $\delta^{15}N$ values (between 7.775 and 12.743‰, mean: 9.752 ± 1.298 ‰) show an inverse pattern (**Figure 2B** and **Supplementary Table 2**). Only punctual increases in TOC are recorded in the lower section; the most significant is at 103 cm (**Figure 2B**). C/S ratio values (0.2–4.35, mean: 1.3 8 ± 1.2) rise in the ≈1927–1979 (35–75 cm) interval, where sediment mean grain size (SMGS) is relatively high (**Figure 2B**). Carbonate content (<16.3%, mean: 10.2 ± 4.2%) increases upward, while IR values (83.7–100%, mean: 89.7 ± 4.2%) show an inverse pattern (**Figure 2A**). $\delta^{13}C$ values (between −26,376 and −22,008‰ mean: −23,495 ± 1.442‰) significantly reduce in the interval where S values (0.18–3.64%, mean: 1.13 ± 0.77%) are at their highest (≈110–75 cm, ≈1882–1927; **Figure 2B**).

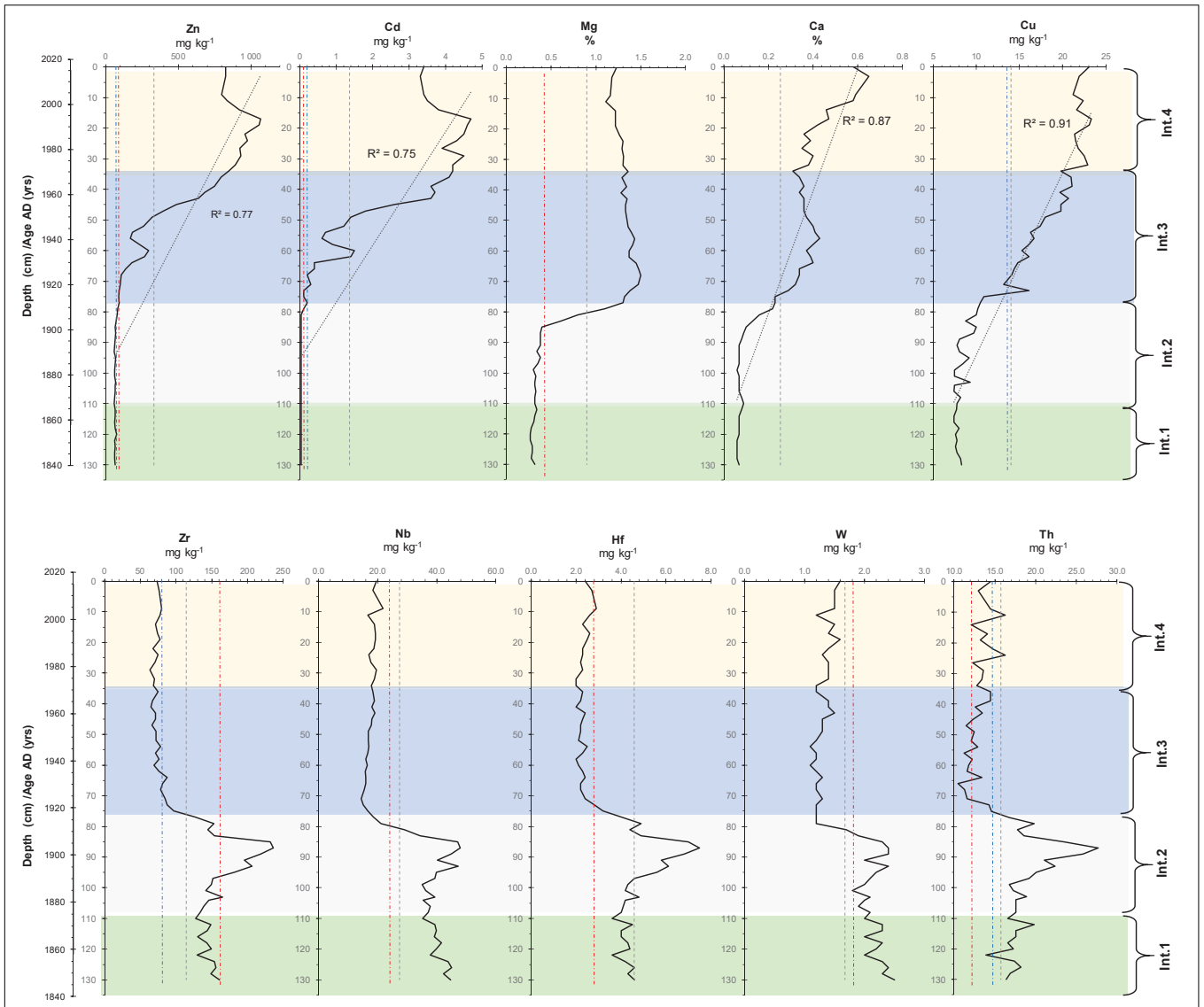

FIGURE 3 | (Continued)

The values and ranges of concentrations of the analyzed elements are included in **Supplementary Table 2**. In some sediment layers, elemental concentrations are above the world shale (Turekian and Wedepohl, 1961; **Table 1**) and local baseline (estimated by Pinto et al., 2019; **Table 1**), such as for Cd, Zn, Mg, and P, which increase in relation to respective baseline values in the upper 70 cm (after 1930; **Figure 3**). The values of Ca and Cu are below the world shale (Turekian and Wedepohl, 1961) and local baseline values (Pinto et al., 2019), but both elements have been showing an increasing trend since ≈1915 (in the upper 75/80 cm; **Figure 3**). It is noteworthy that Ca concentrations are quite low in the inferior part of the core (**Figure 3**). Instead, some elements, such as Zr, Nb, Hf, W, Th, Al, and Ta, reach higher concentrations in the period ≈1858–1927 (130–80/75 cm), but since ≈1927 (above 80/75 cm), their concentrations have been relatively low (**Figure 3**).

Core SP5 has generally higher Pb concentrations than the world shale (Turekian and Wedepohl, 1961) and local baseline values (Pinto et al., 2019; **Figure 3**). Tin (Sn) presents a distribution pattern similar to Pb; both elements decrease their concentrations in the intermediate section where the sediments are coarser (**Figures 2**, **3**). Between ≈1882 and 1927 (≈80/75–110 cm), peaks of U, Mn, Mo, Fe, and S are observed, as well as a sharp decline in P and $\delta^{13}C$ values (**Figures 2**, **3**). In addition to these elements, As concentrations (**Figure 3**) also reach values higher than those of the world shale (Turekian and Wedepohl, 1961) after ≈1965 (in the first ≈40 cm) and local baseline value (Pinto et al., 2019) between ≈1920–1943 (≈80–60 cm).

Some elemental ratios were selected to represent changes in the geochemical composition of the sediments such as: Ti/Ca, which may trace changes in the lithogenic particle supply

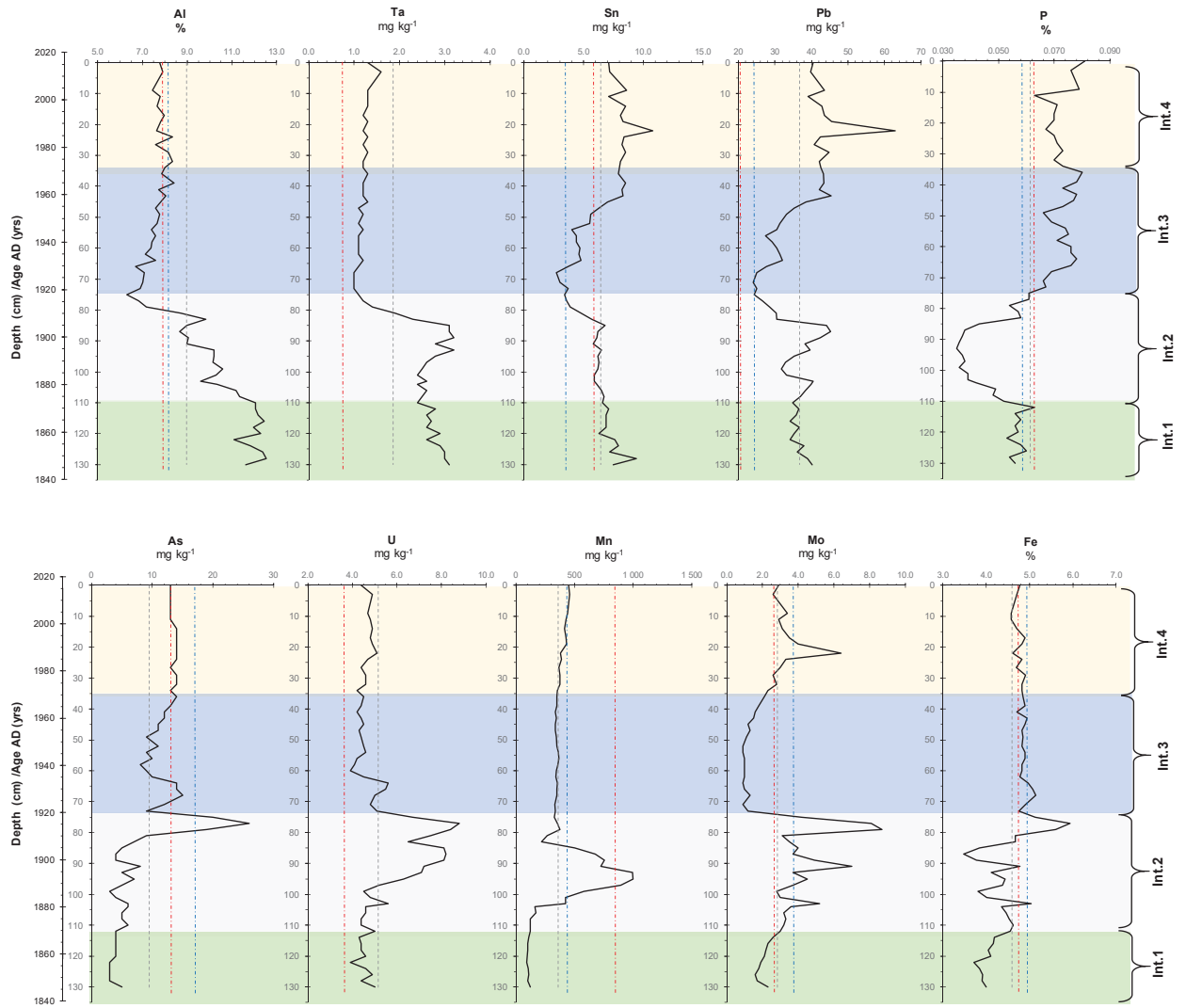

FIGURE 3 | Chemical element concentrations as a function of depth and age (Anno Domini or AD). Based on the analyzed data, four intervals (Int.) are highlighted. Red and blue dashed vertical lines correspond to global baseline values for shale (Turekian and Wedepohl, 1961) and for local fine sediments (Pinto et al., 2019), respectively. Chemical element contents as a function of depth. Based on the analyzed data, four intervals (Int.) are highlighted. Red and blue dashed vertical lines correspond to global baseline values for shale (Turekian and Wedepohl, 1961) and for local fine sediments (Pinto et al., 2019), respectively. The gray dashed vertical line represents the average value for the core.

(Nace et al., 2014; Gebregiorgis et al., 2020); Y/Ni, Cr/V, La/Sc, and Th/Co, which may indicate changes in sources of lithogenic materials in the study area (Hiscott, 1984; Bhatia and Crook, 1986; Cullers, 2002; Okunlola and Idowu, 2012), and Rb/K, which is used to assess changes in water salinity (Campbell and Williams, 1965). Ti/Ca and Th/Co reach higher values in the lower part (below 85 cm), whereas Y/Ni and Cr/V display higher values in the upper 85/90 cm (**Figure 4A**). Rb/K values decrease sharply in the mid part of the core, between 80 and 110 cm. On the contrary, La/Sc ratio shows higher values in this interval characterized by relatively coarser sediments (**Figure 4A**). Changes that occurred in the values of these ratios are discussed.

Considering the classification ranges presented in **Table 2**, EF values are categorized as: $1 < EF < 2$ for Al, As, Fe, P, and Mg; $2 < EF < 5$ for Ce, Hf, Mn, Mo, Nb, Pb, S, Sn, Th, U, W, and Zr; and $5 < EF < 20$ for Zn and Cd (**Supplementary Table 3**). Most of the elements reach maximum Igeo values < 1 (**Supplementary Table 3**), except for Sn and Zr (up to 1), Cd (up to 2.7), and Zn (up to 3.1). The EF and Igeo values of Sn are relatively higher in both ends of the core and decrease in the middle interval where the sediments are coarser. Some elements exhibit maximum CF values > 1, between: 1 and 2 for Al, Th, Hf, Ce, U, Nb, Zr, P, Pb, and Sn, 2 and 3 for Cd, and 3 and 4 for Zn (**Supplementary Table 3**). Higher PERI values (up to 329) are found in the upper core part (**Supplementary Table 3** and **Figure 4B**). The EF and

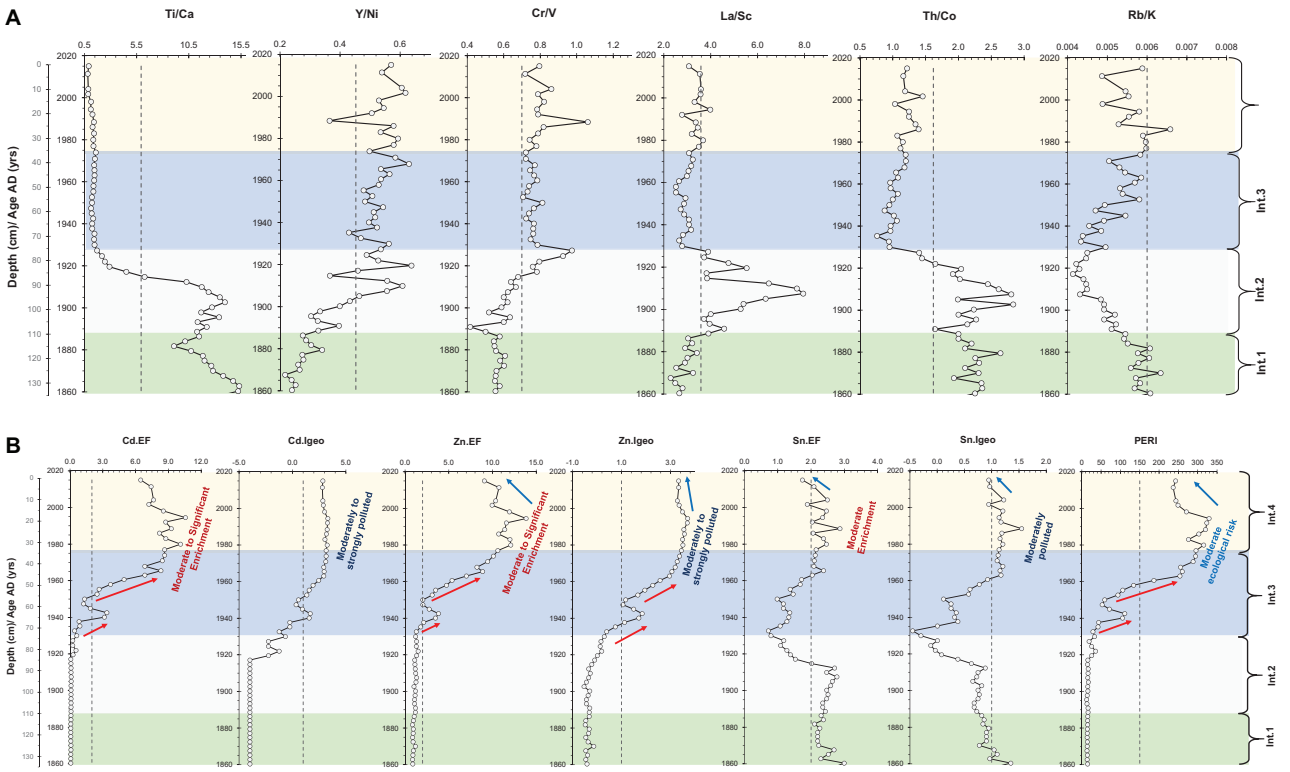

FIGURE 4 | Graphs as a function of depth and age (Anno Domini or AD) of: **(A)** ratios of chemical elements Cr/V, Y/Ni, Ti/Ca, Th/Ca, and Rb/K; **(B)** Igeo and enrichment factor (EF) values for Cd, Zn, and Sn, as well as PERI values. Dashed vertical lines in EF, Igeo and PERI values represent significant values according to **Table 2**: EF > 2 and Igeo > 1. In the PERI graph, the dashed line signals the value of 150, above which ecological risk may be moderate to high.

Igeo values of Cd and Zn and PERI values significantly increase in the upper 80 cm and particularly mostly in the uppermost 50 cm.

Benthic Foraminifera

The FD ranges from 0 to 446 specimens/10 ml (**Supplementary Table 4**). Samples are devoid of foraminiferal tests below 66 cm (**Figure 5**). The highest SR is identified in layers with highest FD. Thirty-eight species are identified along the core, 33 of which have a carbonate test and 5 with an agglutinated test (**Supplementary Table 4**). The most abundant species are *Ammonia tepida, Buliminella elegantissima, Bolivina striatula,* and *Cribroelphidium excavatum* (**Figure 5** and **Supplementary Figure 1A**). *Ammonia rolshauseni*, *Pararotalia sarmientoi*, and *Ammonia parkinsoniana* are also recognized (FD < 19 specimens/10 ml). Other bolivinids and buliminids are identified (density < 10 specimens/10 ml); the abundance of this group increased after 1998. The *Ammonia/Elphidium* index (AEI) shows the predominance of the first group over the second one, with a sharp peak at 30–20 cm depth (**Figure 5**).

In the 0- to 32-cm interval, FD is > 148 specimens/10 ml, and SR varies between 9 and 22 (**Figure 5**). Exp(H'bc) and J' indices ranged between 2.68 and 8.38 and 0.46–0.56, respectively (**Supplementary Table 4**). The most abundant species is *A. tepida*; its frequency is >50% from 1974 and up to 78% (**Supplementary Figure 1B**). This species is followed by *B. elegantissima* (up to 32%) and *P. sarmientoi*, *B. striatula*, and *C. excavatum*. Their abundances do not exceed 6% (**Supplementary Figure 1B**).

The EQR values vary between 0.21 (poor EcoQS) and 0.67 (good EcoQs), with highest values in upper layers of the core (**Figure 6** and **Supplementary Table 5**).

Principal Component Analysis and Canonical Correspondence Analysis Results

The first two PCA components explain about 83% of the total variance (**Figure 7A**). The first component (PC1; ca. 66% of variance) is positively related to C/S, $\delta^{13}C$, coarser grain size (medium + coarse sand), $\delta^{15}N$, Mg, and Fe (**Table 3**). These variables have the highest correlation with the layers deposited around 1943, 1947, 1938, 1953, and 1958, in this order of importance (**Table 4**). Foraminiferal species do not show a positive correlation with these years. PC1 is also negatively related to fine fraction, TOC, and most of the heavy metals (**Figure 5**). Years with highest correlation with these variables are 1974, 1980, 1989, 1998, 2001, 2004, and 2015. Foraminiferal species with highest negative correlation with PC1 are *A. tepida, P. sarmientoi, B. elegantissima, A. parkinsoniana, C. excavatum, B. striatula,* and *A. rolshauseni.* The second component (PC2; ca. 17% of variance) is positively related to K-feldspar and Hf but

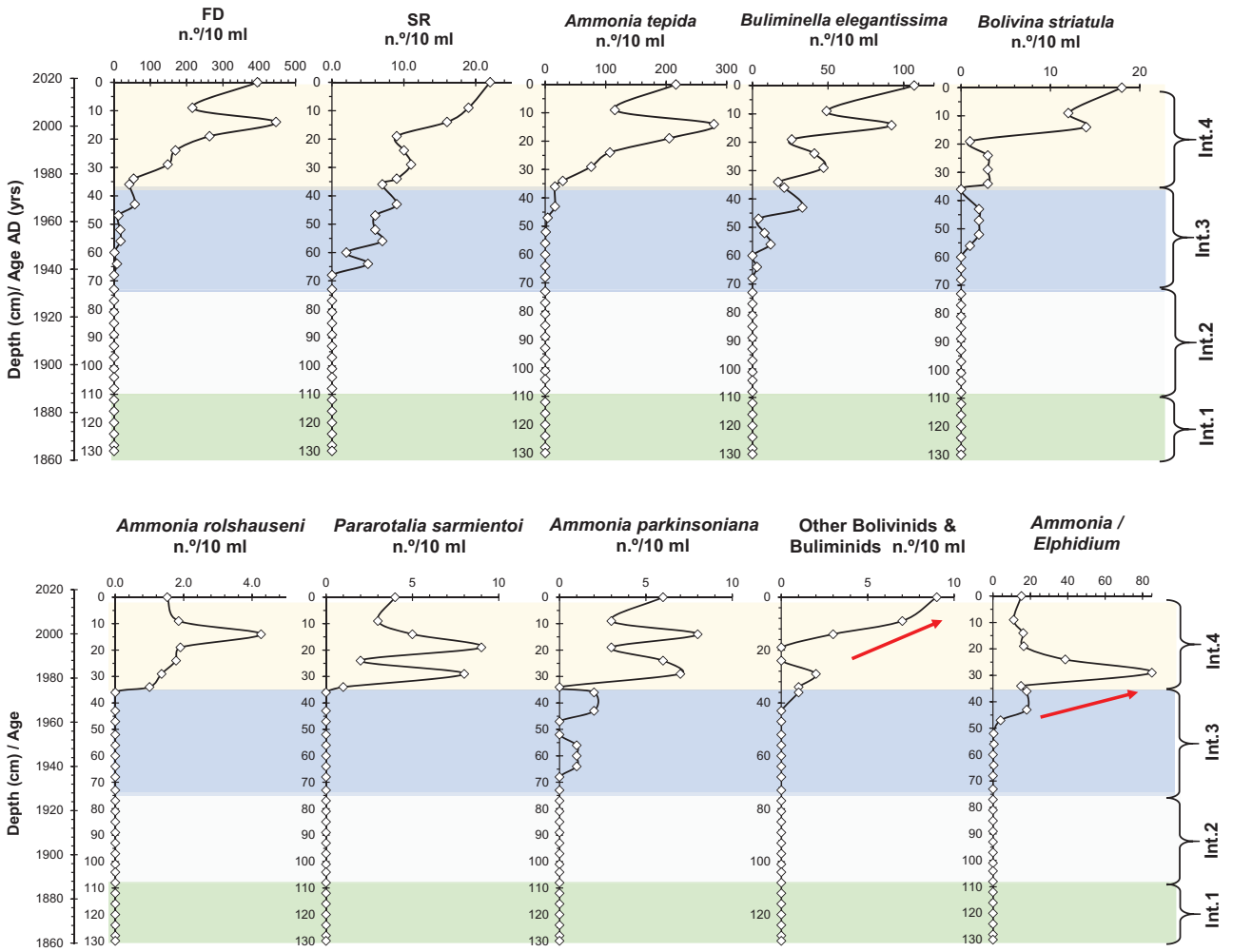

FIGURE 5 | Graphs as a function of depth and age (Anno Domini or AD) of: total benthic foraminiferal density FD) and abundance of several species and taxa, as well as species richness (SR) and *Ammonia/Elphidium* ratio found along core SP5. Based on the analyzed data, four intervals (Int.) were highlighted. The red arrows show a significant increase in the abundance of *Bolivinids* and *Buliminids* and *Ammonia/Elphidium* ratio.

exhibits a negative correlation with Al (**Table 3**). *Bolivina striatula* and *C. excavatum* are correlated with the period around 2004. Foraminiferal species do not have a significant correlation with the negative axis of PC2.

The CCA results for axes one and two (explaining 56.5 and 11.3%, respectively, of data variability) represent the main relationship of species with selected sedimentological variables and samples represented by decades (**Figure 7B**). The positive side of axis 1 is mostly related to PERI, La/Sc, fine fraction, TOC, C/N, and the species *P. sarmientoi, A. tepida*, and A. *rolshauseni* and the decades 1980s, 1990s, and 2000s, while its negative side contains the species *A. parkinsoniana, B. elegantissima, C. excavatum,* and *B. striatula,* the sedimentological variables Ti/Ca, $\delta^{13}C$, $\delta^{15}N$, and C/S, and the decades 1940s, 1950s, 1960s, 1970s, and 2010s. Axis two separates the species *A. parkinsoniana, B. elegantissima*, and *P. sarmientoi* (positive side) *from C. excavatum, B. elegantissima,* and *A. rolshauseni* (negative side), and associates the first group with most of the sedimentological variables and the second group with the 1940s, 1950s, 2000s, 2010s, and the gradients of TOC and C/N ratio.

DISCUSSION

Relatively high sediment accumulation rates in the study area provide good discrimination of past natural/anthropic processes (Castelo et al., 2021a). The mean sediment accumulation rate estimated in core SP5 was $\approx 0.83 \pm 0.13$ cm year^{-1}. Similar values have been found by other authors (e.g., Barcellos et al., 1997; Marques et al., 2006). Castelo et al. (2021b) documented higher values ($\sim 1.36 \pm 0.05$ cm year^{-1}) of sediment accumulation rates in a core (SP3) located in the most central area of the bay. Gonçalves et al. (2020) obtained much lower values (e.g., from 13 cm year^{-1} before the 1980s to 0.255 cm year^{-1} after this period) in the eastern region of the bay, near Guaratiba. Borges and Nittrouer (2016a,b) suggested that the average

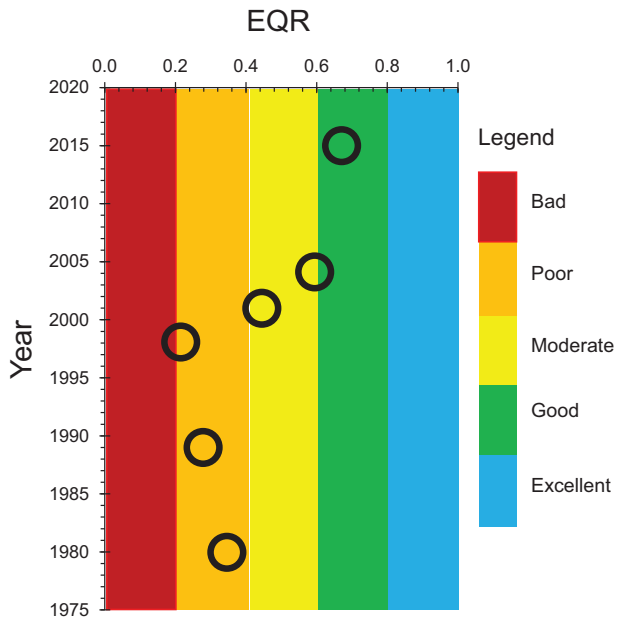

FIGURE 6 | Ecological Quality Ratio (EQR) in core SP5 as a function of year. The classification of EQR values (in accordance with Van de Bund and Solimini (2007) are shown.

sediment accumulation rate in the bay varied from the Holocene transgression period to a part of the last century. According to these authors, during this period, sediment accumulation rate in the bay was <0.17 cm year^{-1}, significantly increased during the 1970s (~0.37 cm year^{-1}), and in the last 20 years the region has achieved even higher sediment accumulation rates ranging from 0.1–2 cm year^{-1} in muddy areas to 0.4–1.2 cm year^{-1} in tidal flats. Borges and Nittrouer (2016a,b) suggested that the increase in sedimentation in the last 20 years was related to the accumulation of muddy sediments in the northwestern part of the bay and consequent progradation of the coastline since 1868. Barcellos et al. (1997) noticed higher accumulation rates in the estuarine area, which is north of the bay, than in the outer sector, which is related to Guandu River delta changes (recognized by Borges and Nittrouer, 2016a).

Changes in the Sedimentary Environment

The mineralogical and geochemical results reveal that the sediments of core SP5 are essentially siliciclastic. Chromium (<110 ppm) and Ni (<65 ppm) concentrations (**Supplementary Table 2**) are below the North American shale composite values (NASC; Garver et al., 1996) and indicate that the main source of the sediments are felsic rocks (Hossain et al., 2017). The La/Sc vs. Th/Co diagram (**Figure 8A**) based on Cullers (2002) and Okunlola and Idowu (2012), the Zr-Th-Sc ternary diagram (**Figure 8B**) based on Bhatia and Crook (1986) and Okunlola and Idowu (2012), and the Hiscott diagram (Hiscott, 1984) of Cr/V vs. Y/Ni (**Figure 8C**) also point out a metamorphic felsic origin as main source of the sediments. This is in accordance with the geological evolution and lithological composition of this region (Heilbron et al., 2020).

The variation of concentrations of some chemical elements is positively correlated with the fine fraction of the sediments (such as Al, Bi, In, Nb, Ta, Ti, V, and U; **Supplementary Table 6**), indicating variations in the fluvial contribution of eroded materials from the drainage basin to the study area, as also observed by Gonçalves et al. (2020). The increase in concentrations of these chemical elements may reflect calmer hydrodynamic conditions favorable for fine sediment accumulation. However, some chemical elements such as Cd, Cr, Cu, Ni, P, and Zn show non-significant correlations with fine sediments (**Supplementary Table 6**) and may be associated with pollutant sources related to anthropic activities developed in the region (Magalhães et al., 2001; Mounier et al., 2001; Molisani et al., 2004; Araújo et al., 2017a,b). Other elements, such as As, Be, Ca, Ce, Co, Fe, Mg, Mn, Na, Rb, Sr, U, and Y, are significantly and positively correlated with sand fraction (**Supplementary Table 6**). These results suggest that natural/anthropogenic processes may influence the compositional characteristics of sediments in the study area.

Thus, in order to be able to characterize possible changes in sediment characteristics and associate them with possible causes, four main intervals were considered along core SP5:

1. Interval 1 (Int. 1), between ≈1858 and 1882 (≈133–110 cm), is characterized by polymodal and poorly sorted fine-grained sediments, relatively low TOC (around 0.5%), N, carbonate (generally < 10%), pyrite, and feldspars/quartz values, and by low concentrations of Zn, Cd, Mg, Ca, and Cu. In contrast, it is marked by relatively high δ^{13}C values and concentrations of, for instance, Zr, Nb, Hf, W, Th, Al, Ta, and IR, and is devoid of foraminiferal, mollusk, and ostracod remains.
2. Interval 2 (Int. 2), between ≈1882 and 1925 (≈110–75 cm), is distinguished mainly by accentuated decrease in δ^{13}C values; it has geochemical characteristics (e.g., Zn, Cd, Mg, Ca, Cu, N, C/S, and TOC values) similar to those of Int. 1, but it shows a sharp increase in Zr, Nb, Hf, W, Th, Ta, Pb, S, and SMGS (due to rise of medium to coarse sand fractions of sediments). It is also denoted by overall decrease in Al and fine fraction, sharp reduction in P, peaks of As, V, Mn, Mo, Fe, δ^{15}N, and C/N, and, again, absence of foraminifera.
3. Interval 3 (Int. 3), between ≈1925 and 1974 (≈75–34 cm), is characterized by presence of sandy sediments, but SMGS starts to decrease. It is also marked, for example, by increasing trend in TOC, N, Zn, Cd, and Cu, relatively high values of δ^{13}C, Mg, Ca, carbonates, and P, abrupt rise in C/S ratio values, reduction in IR and δ^{15}N, relatively low concentrations of Zr, Nb, Hf, W, Th, Al, and Ta, and presence of foraminifera in the sedimentary record.
4. Interval 4 (Int. 4), between ≈1974 and 2015 (≈34–0 cm), is marked by significant increase in FD, occurrence of fine-grained sediments, relatively high values of TOC, N, Zn, Cd, Cu, δ^{13}C, Mg, Ca, carbonates, and P, and relatively low values of Zr, Nb, Hf, W, Th, Al, Ta, RI, C/S, and δ^{15}N.

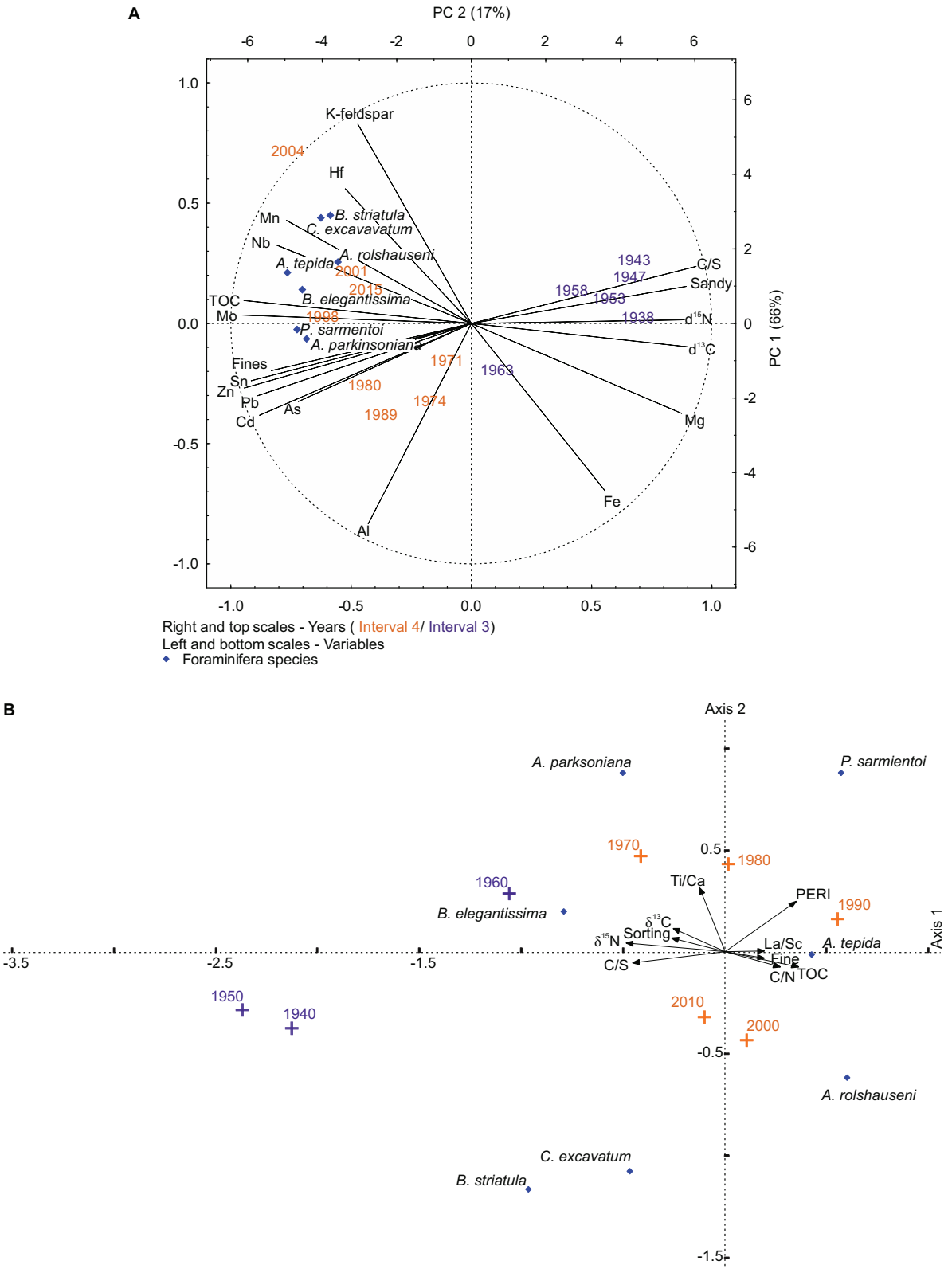

FIGURE 7 | (A) PCA ordination diagram plotting the primary (sediment parameters) and secondary (foraminiferal species) variables as well as layers (years). **(B)** Canonical correspondence analysis (CCA) showing the relationship among the species, selected sedimentological variables, and samples represented by decades. PERI, potential ecological risk index; Fine, fine fraction.

The geomorphology of the bottom of the SB is complex and has changed considerably over time, as shown in studies of Friederichs et al. (2013) and Reis et al. (2020). The compositional characteristics of the sediments of Ints. 1 and 2 may have resulted from Guandu River delta processes and/or changes in geomorphological characteristics of the study area, as suggested by its sedimentological characteristics. Araripe et al. (2011) suggested that the elements Hf and U are associated with the mineral zircon, which is a possible product of erosion of igneous rocks located in surroundings of the bay. Thus, the increased concentration of these elements in Int. 2 indicates that the supply of materials is mainly from continental provenance. In fact, the high values of Ti/Ca ratio (**Figure 4**) coupled with relatively high concentrations of Zr, Nb, Hf, W, Th, Al, Ta, and IR observed in Ints. 1 and 2 (**Figure 3** and **Supplementary Table 2**) also indicate the accumulation of essentially lithogenic particles (Nace et al., 2014; Gebregiorgis et al., 2020) and presence of a quite low biogenic component, as supported by low carbonate contents, and absence of mineralized foraminiferal tests (**Supplementary Table 4**), ostracods, and mollusks. The poor preservation of biogenic carbonates should be caused by low pH conditions. It should be noted that foraminiferal tests start dissolving when the pH decreases to values below 7.6 (Prazeres et al., 2015). The pH decrease may have resulted from organic matter degradation processes and from acid percolation through the sedimentary column. However, carbonates were still identified in these intervals (**Figure 2**); since not only $CaCO_3$ but also other types of carbonates with differentiated resistance to dissolution by acids should be present.

TABLE 3 | Correlations between factors and variables (factor loadings) based on the inverse matrix (product-moment/Pearson).

Variable	PC1	PC2
Fine Fraction	−0.83	−0.20
Sand Fraction	0.89	0.15
K-Feldspar	−0.47	0.83
TOC	−0.95	0.10
C/S	0.94	0.24
$\delta^{15}N$	0.89	0.02
$\delta^{13}C$	0.90	−0.10
Al	−0.43	−0.83
As	−0.72	−0.33
Cd	−0.88	−0.38
Fe	0.56	−0.70
Hf	−0.53	0.56
Mg	0.88	−0.38
Mn	−0.77	0.43
Mo	−0.96	0.04
Nb	−0.81	0.33
Pb	−0.89	−0.30
Sn	−0.92	−0.24
Zn	−0.95	−0.27
A. parkinsoniana	−0.69	−0.07
A. rolshauseni	−0.56	0.26
A. tepida	−0.76	0.21
B. striatula	−0.59	0.45
B. elegantissima	−0.70	0.14
C. excavatum	−0.63	0.44
P. sarmientoi	−0.73	−0.03

TABLE 4 | Factor 1 and factor 2 of the PCA included in **Figure 7A** as a function of years from intervals 1 to 4 (based on correlations).

Year	Factor 1	Factor 2	Interval
2015	−2.80146	0.65347	Int. 4
2004	−4.89353	4.37483	Int. 4
1998	−3.16929	1.14847	Int. 4
1992	−3.97262	−0.05838	Int. 4
1986	−2.55022	−2.05900	Int. 4
1980	−2.60439	−2.03930	Int. 4
1974	−1.07882	−2.32842	Int. 4
1971	−0.33479	−1.32120	Int. 3
1963	0.46860	−1.53466	Int. 3
1958	2.72534	0.63474	Int. 3
1953	3.74399	0.42714	Int. 3
1947	4.90262	0.94679	Int. 3
1943	5.04476	1.25013	Int. 3
1938	4.51980	−0.09462	Int. 3

Int., interval.

These geochemical data indicate that the sediments are mostly supplied by the erosion of local and regional rocks. However, the reduction in La/Sc and Th/Co values and higher values of Y/Ni and Cr/V ratios (Hiscott, 1984) in Ints. 3 and 4 (**Figure 4**), reveal a greater occurrence of mafic and ultramafic rocks in the composition of the sediments, which may be related to changes in the characteristics of sedimentary dynamics in the region. Despite the expressive record of lithogenic supply in core SP5, the mineralogical results also suggest changes in proximity to the source area of the sediments or changes in reworking processes, mostly in Int. 4. The higher values of feldspars/quartz ratio in Int. 4 (**Figure 2**) may indicate higher sedimentary input from the drainage network adjacent to the study area and presence of less weathered sediments, since minerals from the feldspar group are less resistant to weathering than quartz (Lira and Neves, 2013). This change may be due to the natural evolution of the SB, but it may also have been influenced by anthropic actions.

Population increase (and related activities) in the river margins (Barcellos et al., 1997; Borges and Nittrouer, 2016a,b) may have facilitated the transport of less reworked sediments to the study area. Exploration of sand in the river margins have promoted disfigurement of the river channels and collapse of the margins, which generated holes and lateral creeks (SEMADS, 2001) and enhanced the greater contribution of sediments of continental origin to the study area (Barcellos et al., 1997). On the other hand, sediments from the lower part of the core (Int. 1 to Int. 3) have relatively low feldspars/quartz ratios, indicating that the sediments have undergone greater reworking than those from Int. 4.

Transitional waters are normally exposed to both continental drainage and marine action (Perillo, 1995). Changes in continental/oceanic influence were inferred from Rb/K ratio. This ratio has been used to interpret varying levels of salinity

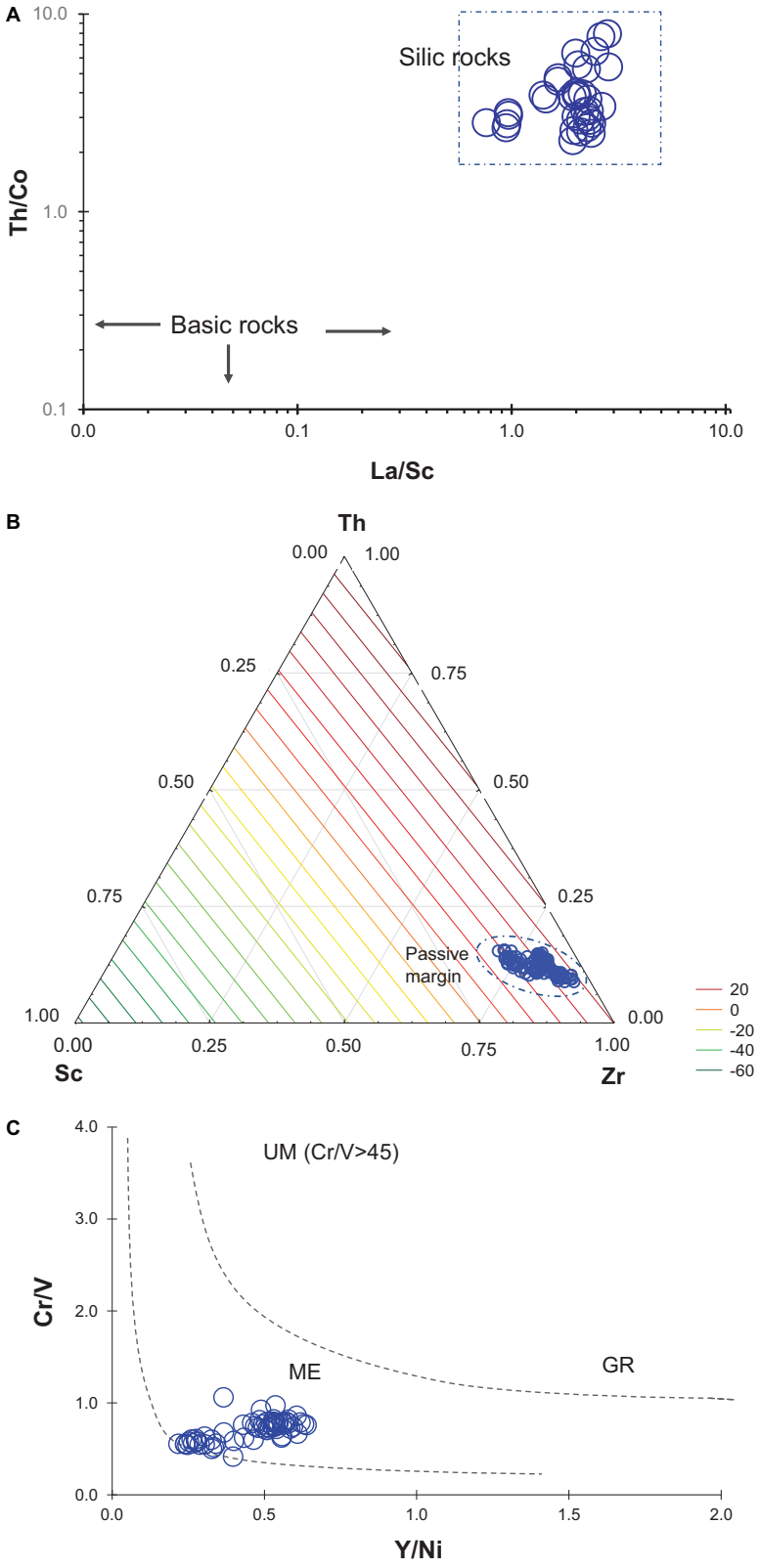

FIGURE 8 | (A) Biplot of La/Sc vs. Th/Co ratio based on Cullers (2002) and Okunlola and Idowu (2012). **(B)** Zr-Th-Sc ternary diagram based on Bhatia and Crook (1986) and Okunlola and Idowu (2012). **(C)** Hiscott diagram (Hiscott, 1984) of Cr/V vs. Y/Ni, indicating ultramafic (UM), metamorphic felsic (ME), and granitic (GR) rock fields.

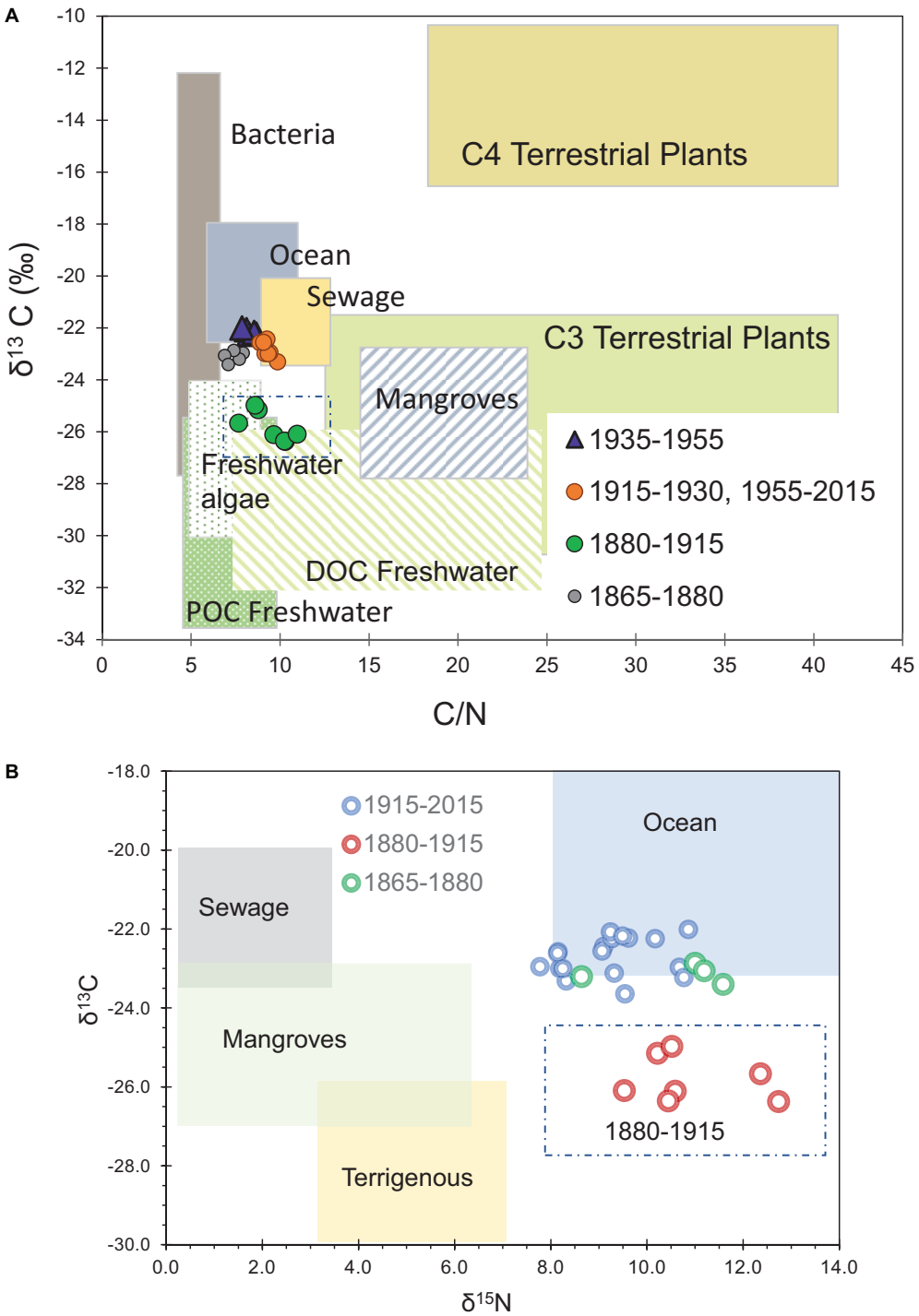

FIGURE 9 | Graph of the values of: **(A)** $\delta^{13}C$ against C/N ratio and **(B)** $\delta^{13}C$ against $\delta^{15}N$. The suggested fields are based on Deines (1980), Lamb et al. (2006), Martinelli et al. (2009), Barros et al. (2010), and Bueno et al. (2019). Points are levels analyzed in the SP5 core. DOC, dissolved organic carbon; POC, particulate organic carbon. The values for the period registered in the SP5 core between 1880 and 1915 were marked in blue dashed lines.

(Liu and Cao, 1984; Wang et al., 2016; Zou et al., 2021) as the following: (1) Rb/K ratio of ≤0.004 indicates freshwater conditions; (2) > 0.004 to ≤ 0.006 suggests influence of fresh to brackish water, and; (3) > 0.006 fully marine conditions (Campbell and Williams, 1965). The use of this ratio along core SP5 is based on the assumption that fine marine sediments contain higher Rb contents because of increased concentrations of this element in seawater (0.12 ppm) compared to freshwater

environments (0.0013 ppm). Potassium concentrations in core SP5 are positively correlated with sandy sediments (with higher proportion of fine, medium, and coarse sand; **Supplementary Table 6**), as their highest concentrations were reached in coarser sediments (**Figure 3**), as well as Rb concentrations (**Figure 3**). K concentrations can be associated with several mineral types such as K-feldspar ($KAlSi_3O_8$), mica ($Kal_2Si_3AlO10(OH)_2$), and illite ($K,H_3O)(Al, Mg, Fe)2(Si, Al)4O10[(OH)2,(H_2O)]$. The data obtained by Pinto et al. (2019), along core SP2 and collected near the mouth of Guandu river (22°55′0.00″S; 43°45′60.00″W), reveal that the main clay mineral is illite (45–74%). Thus, K concentrations may represent a lithic component consisting of K-feldspar and phyllosilicates. Thus, the reduction of Rb/K ratio values in Int. 2 (**Figure 4**) likely suggests the influence of less saline water. This inference is also supported by the stable isotope results of organic matter, as explained below.

The plot of $\delta^{13}C$ vs. C/N (**Figure 9A**) and $\delta^{13}C$ vs. $\delta^{15}N$ (**Figure 9B**) and the values and ranges suggested based on Deines (1980), Lamb et al. (2006), Martinelli et al. (2009), Barros et al. (2010), and Bueno et al. (2019) allow us to infer that the study area received a contribution of organic matter from several sources, including terrestrial C3 plants, freshwater algae, oceanic productivity, and sewage discharge (**Figure 9**). The most negative $\delta^{13}C$ values (Meyers, 1997) may be related to greater supply of an organic material of fresh water algae origin. This corroborates the inference regarding lower Rb/K values, which indicate higher freshwater influence in the study area (**Figure 4**). However, the fact that these more negative values are simultaneously recorded with higher levels of S and slight increase of pyrite (**Figures 2A,B**) allows us to deduce that they may have also been influenced by diagenetic changes in the sediment, which led to the production of sulfides in anoxic sedimentary sub-environments. On the other hand, according to Stein (1991), $\delta^{13}C$ values around -20‰ may be related to marine plankton. Thus, the less negative values of $\delta^{13}C$ recorded between ≈1930 and 1955 associated with lower values of C/N ratio may represent higher contribution of organic matter from marine productivity and between ≈1960 and 2015 associated with relatively high values of C/N ratio, which should indicate greater contribution of sewage to the study area. This is also evident in increased TOC values since ≈1963 (45–0 cm; **Figure 2**).

In fact, highest TOC contents reaching ca. 1.8% are found in Int. 4, associated with fine grained sediments (**Figure 2** and **Supplementary Table 2**). However, as TOC concentrations can reach up to 12.5% in coastal areas influenced by human activities, such as domestic or industrial sewage discharges (Kennish, 1997), this enrichment can be considered as moderate. TOC contents are, in general, <0.8% before ≈1930, which may indicate low organic matter preservation and/or high heterotrophic activity and/or remobilization after deposition (Souza et al., 2017). However, the presence of pyrite in Int. 1 and Int. 2 and along the entire core (**Figure 2** and **Supplementary Table 2**) indicates low oxic conditions of the sediments, even in the sandiest layers. This mineral is formed in anoxic sediments, and its preservation also occurs in oxygen-depleted environments (Wang and Morse, 1996).

The prevailing low-oxygenated conditions are also corroborated by the low values of C/S ratio. According to Lyons and Berner (1992), C/S ratios below 2.8 ± 0.8 indicate sediments deposited under reducing conditions. Most part of this core has C/S values <2.8. However, a peak of C/S ratio occurs in the middle part of the core (Int. 3), which is associated with coarser grained sediments (**Figure 2**) indicating the presence of more "oxic" sediments when compared to another interval, namely, the Int. 1. However, the presence of oxic boundaries is already noticed in the previous interval (Int. 2) through the increase in redox-sensitive elements, such as U, Mn, Mo, S, and Fe (e.g., Urban et al., 1999; Brown et al., 2000; Zheng et al., 2000, 2002; Adelson et al., 2001; Thomson et al., 2001). The high enrichment of these metals is usually attributed to changes in redox conditions of the sediment. Thus, the increase in redox-sensitive metals, especially U and Mn, depletion of Ti/Ca values associated to coarser sediments, and grain size indicate strengthening of hydrodynamics in Int. 2, probably because of higher connection of the study area with oceanic waters. Increased marine influence may have been favorable to the development of carbonate-bearing organisms, especially foraminifera, which led to progressive enrichment of biogenic carbonates from Int. 3 onward.

In summary, the results presented reveal that:

1. The main sources of sediments supplied to the study area were mainly felsic metamorphic rocks;
2. The fluvial contribution of eroded materials from the drainage basin was more intense in Ints. 1 and 2, with higher contributions of materials supplied mainly from continental provenance, especially in Int. 2, a period when hydrodynamic conditions seemed to have been more active in the studied site;
3. Int. 2 may have been more influenced by more freshwater and organic matter from river sources;
4. The textural and compositional characteristics of the sediments in Ints. 1 and 2 may reflect processes associated with the Guandu River submarine delta;
5. The sediments have become enriched in mafic minerals in Ints. 3 and 4 probably because of changes in sediment dynamics, also favorable to the accumulation of organic-rich fine sediments; and
6. Circulation conditions similar to the present ones were established from Int. 3 onward, with prevalence of calmer conditions, which favored the accumulation of carbonate shell/test benthic fauna.

Impact Caused by Anthropogenic Influence

On the basis of the EF values and classification criteria of Sutherland (2000), Int. 4 has sediments moderately to significantly enriched in Cd, Zn, and Sn. Similarly, the Igeo values and Müller's (1986) classification criteria suggest moderately to heavily polluted conditions by these PTEs in this interval. Contamination with the Cd and Zn metals is widely documented in the study area (e.g., Lacerda et al., 2001; Mounier et al., 2001; Martins et al., 2019; Castelo et al., 2021a,b). Companhia Ingá

Mercantil (or CIA Ingá, currently inactive) may have significantly contributed to this situation. This company, founded in the 1950s in Madeira Island (**Figure 1**), was responsible for the production of high-purity zinc (Magalhães et al., 2001; Mounier et al., 2001; Molisani et al., 2004; Araújo et al., 2017a,b). The liability generated by CIA Ingá was the target of several tailing leaks, such as what happened in February 1996 where 50 million L of contaminated water and mud were dumped into the SB (Melo, 1996). However, Cd and Zn concentrations tended to decline at the top of core SP5 after the inactivity of CIA Ingá in 1997 (Fundação Estadual de Engenharia do Meio Ambiente [FEEMA], 1997; Molisani et al., 2004).

Araújo et al. (2017a,b) found higher concentrations of Zn and Cd than this study in areas close to Cia Ingá. This suggested the presence of internal vertical flows that promote remobilization of fine particles, enhancing the dispersion of metals and resuspension and transport of sediments contaminated along the bay. It is possible that the presence of these contaminants in core SP5 has resulted from the dispersion of pollutants from the source areas. Sediment destabilization through ship traffic, heavy swell, and dredging operations in navigable channels to give access to the Sepetiba/Itaguaí port may have released contaminants to the water column. These contaminants were transported by currents to the study area and several other areas.

Tin concentrations are relatively higher at the top and the lower part of core SP5 (**Figure 3**) but decrease in the middle zone of the core (in coarser sediments; **Figure 2**). However, this change does not fully accompany changes in sediment grain size and may be related to lithogenic sources of the metals. In addition, the increase of Sn concentration in the upper part of core SP5 may also be a consequence of anthropogenic contributions. Tin contamination in the upper part of this core may be also associated with two main sources: use of biocides such as tributyltin (TBT) and ore deposits of cassiterite. Ban on the use of paints with antifouling properties based on TBT started in Europe and Asia during the 1970s and 1980s (Alzieu, 2000). However, restriction in the use of TBT only occurred in Brazil in 2007 (NORMAM-23/DPC, 2007). The overall decline of this biocide toward the top of the core may probably be attributed to this restriction. The main source of Sn in Brazil is cassiterite. There are important reserves of cassiterite in Rondônia, northern Mato Grosso, southern Amazonas, and southern Pará where exploitation of this element is important (White, 1974). Minor deposits or occurrences of cassiterite are located in Pará, Amapa, Paraiba, Rio Grande do Norte, Ceará, Bahia, Minas Gerais, Goiás, São Paulo, and Rio Grande do Sul (White, 1974). Ore materials transported from other regions of Brazil are refined and metallurgically treated at Companhia Estanífera do Brasil near a steel plant, Brazilian government's National Steel Mill, in Volta Redonda (Rio de Janeiro State), about 60 km from Sepetiba, which has been in operation since the 1950s (Rogers, 1968; Warhurst, 1999). This activity should be also a source of this chemical element for SB. Studies have revealed that dispersion of Sn from this alloy industry through the atmosphere (wind transport of particulates) has been important in the region and is causing serious public health problems (Azevedo et al., 2019). In addition, there are lithologies containing stanniferous deposits or occurrences associated with, for instance, Funil Granit, located in the Resende Basin, Rio de Janeiro (Pereira et al., 2003), which is about 85 km from the SB. Therefore, the presence of Sn-enriched lithologies in the region should also be a source of this chemical element.

Phosphorus contents increased in Int. 3 and remained relatively high (generally above the local and world shale baseline values) in Int. 4 (**Figure 3**). Phosphorous has significant positive correlations with TOC, carbonates, and several metals, such as As, Ca, Cd, and Zn, but not with pyrite (**Supplementary Table 6**). This is due to the fact that the relative abundance of this mineral is generally lower in the upper section of the core, since it is the least depleted in oxygen. This suggests that the increase in P in Int. 3 and Int. 4 may have been influenced by municipal sewage, diffuse (fertilizers) runoff from agricultural soils, and its increase should be also related to sources of pollution. Phosphorus is a chemical element that acts as a nutrient for phytoplankton and facilitates the reproduction of algae and vascular plants, contributing to the eutrophication process (Schauser et al., 2004), that is, high supply of organic matter to the bottom. Castelo et al. (2021a) suggested that the supply of organic matter favored sub-oxic conditions in the region, and that the occurrence of pyrite was the result of the anoxic condition in the bay's microenvironments contributing to retention of PTEs.

High concentrations of As in the vicinity of Madeira Island have been previously reported by Magalhães and Pfeiffer (1995) (**Figure 1**). The relatively high concentrations of As recorded in core SP5 in Ints. 3 and 4 (**Figure 3**) can be associated with high-purity Zn and Cd treatment process by metallurgical companies in the region (Barcellos et al., 1991). However, the highest enrichment of As recorded in core SP5 occurred in Int. 2 (**Figure 3**) before the aperture of CIA Ingá. Therefore, this enrichment is also probably associated with lithological sources and to the weathering of the rocks of the region (as also observed by Pinto et al., 2019).

Arsenic is rarely found as a native element because of its binding affinity for other elements and mineral species except hydrothermal ores (Reimann et al., 2009). It can form As^{3+} oxides, arsenolite, and claudetite (both As_2O_3), polymorphs with similar thermodynamic stability (Nordstrom and Archer, 2003). These minerals can form products of arsenic sulfides (AsFeS) occurring primarily in hydrothermal and magmatic ore deposits (O'Day, 2006). Relatively high concentrations of As have been found in beach sand from Espírito Santo and Rio de Janeiro states (Mirlean and Baisch, 2016). The presence of relatively high concentrations of As in these coastal regions is still very poorly understood but has been attributed to various geochemical processes such as early diagenetic processes (Mirlean and Baisch, 2016) and hydrothermal vents associated with past magmatic activity (Heilbron et al., 2020). In this region, As, on average, is about 30 times higher than the background value for sandy sediments and 10 times higher than the background value in near shore mud (5 mg/kg) (Mirlean and Baisch, 2016). High As concentrations were also found in shallow groundwater in the Paraíba do Sul delta (N of the study area) probably as a result of release of As bound by authigenic sulfides (Mirlean and Baisch, 2016). The rate of oxidation of sulfides depends on several factors,

including amounts of arsenopyrite (e.g., AsFeS), particle size distribution, temperature, and time of exposure of the material to atmospheric water and oxygen (O'Day, 2006).

The data of core SP5 suggest that many natural and anthropogenic factors may have caused the enrichment of some chemical elements. However, the sediment enrichment in PTEs in the inner SB area since the 1950s, but especially since the 1970s, may have been associated primarily with anthropogenic forcing.

Recent Evolution of the Study Area

The absence of foraminifera between ≈1858 and 1925 suggests that the natural environmental conditions in the study area were not suitable for the presence of these organisms during Int. 1 and Int. 2. The sediments deposited in this period were also characterized by low Ca concentrations, which corroborates the absence of foraminifera and mollusk shells. Note that the presence of carbonates (more regularly in Int. 2) may indicate favorable conditions for the formation of these minerals by abiogenic processes and/or their transport and accumulation in the study area. According to Silva et al. (2000), precipitation of evaporitic minerals occurs in a predictable order, as salt water evaporates, with calcite being the first mineral to be deposited. In fact, during the ≈1882–1925 interval, this area of the bay should have been associated with processes of the deltaic complex of Guandu River. The site where core SP5 was collected was in an elevated region and, therefore, must have gone through phases of subaerial exposure, periods of greater freshwater influence, alternating with other phases in which the area was invaded by marine waters. These phases favored the precipitation of inorganic carbonates. However, such conditions were not favorable to the establishment of benthic foraminiferal communities.

With the establishment of oceanic circulation similar to the present one, the study area became progressively more suitable for the development of benthic foraminifera. Starting from ≈1938 (Int. 3 to Int. 4), foraminifera appeared in the sedimentary record (**Supplementary Table 4** and **Figure 5**). The large variability of the physicochemical parameters and the instability of the substrate prevented the significant development of a stable community in the study area in Int. 3 (≈1935–1974). In this interval, the assemblages were affected by the extreme complexity of the hydrodynamics, with large asymmetries in the distribution of ebb-flood currents caused by the semi-diurnal variation of tides and friction with bed forms (Cunha et al., 2006). These conditions could have generated the polymodal and very poorly sorted sediments of Int. 2 and Int. 3.

The prevalence of calm hydrodynamic conditions in Int. 4 after ≈1974 (**Figure 5**), combined with abundant food supply, allowed for increase in benthic foraminifera abundance. However, only poorly diversified assemblages were recognized. Mainly species with opportunistic behavior, such as *A. tepida, B. elegantissima, B. striatula*, and *C. excavatum*, common in anthropized coastal environments, as has been noticed in previous studies (e.g., Duleba and Debenay, 2003; Vilela et al., 2004; Alves Martins et al., 2019b; Castelo et al., 2021a).

Ammonia tepida is a common species in coastal environments because of its tolerance to physicochemical variations such as in salinity, temperature, and nutrient availability (Zaninetti et al., 1977; Bouchet et al., 2007; Frontalini et al., 2009). The relatively high values of *Ammonia/Elphidium* ratio in Int. 4 indicates a shallow confined transitional environment. According to Duleba et al. (2018, 2019), the highest proportion of *Ammonia* spp., in relation to *Elphidium* spp., suggests the presence of stressful coastal environmental conditions due to bottom water and/or sediment pore water hypoxia. Thus, the highest values of the AEI in Int. 4 indicate a progressive trend toward the occurrence of eutrophication and consequent reduction in oxygen associated with the presence of sediments with moderate to considerable ecological risk, according to PERI values.

The enrichment of PTEs (namely, Cd, Zn, and Sn) seems to have been a conditioning factor for the establishment of diversified assemblages and the presence of species sensitive to these adverse environmental conditions. Along the core, the most abundant species (*A. tepida, B. elegantissima, B. striatula*, and *C. excavatum*) are known to be tolerant to high instability of transitional waters and presence of high TOC, low oxygen contents (Brönnimann et al., 1981; Murray, 1991, 2006; Moodley and Hess, 1992; Alve and Murray, 1999; Frontalini et al., 2009), and even metal-induced pollution (Vilela et al., 2004).

The PCA results and isotope data (**Figures 7A**, **9**) show that the increased density of most frequent species in foraminiferal assemblages found in the upper part of core SP5 is associated with increase in organic matter of mixed sources, including those of marine and land origin materials, in addition to calm hydrodynamic conditions. Although these assemblages were found in sediments moderately to strongly polluted mainly by Cd and Zn, factor 2 of the PCA (**Figure 7A**) shows that the higher abundance of these organisms is reached in less polluted sediments by PTEs. However, it is not the abundance of foraminifera that shows the quality of the environment but the composition and diversity of their assemblages, which are related to the response of the species to environmental stress (Alves Martins et al., 2020). The high metal content and amount of organic matter, and the redox state of the sediments are conditioning factors of the type of foraminiferal assemblages found in the study area. However, the quality of the organic matter also seems to be an important factor. Some species, such as *A. parkinsoniana, B. elegantissima, C. excavatum*, and *B. striatula,* are mostly related to better quality of organic matter (as indicated by the higher $\delta^{13}C$ and $\delta^{15}N$ values) related to marine productivity.

PaleoEcoQS was poor in 1975, highlighting the impact of anthropogenic activities. They worsened after the metal spill event from CIA Ingá that occurred in 1996 (Melo, 1996; Magalhães et al., 2001; Mounier et al., 2001; Molisani et al., 2004). Since then, environmental quality progressively improved, and PaleoEcoQS became good in 2015. Hence, our results indicate a possible trend for recovery of the study area after more pronounced environmental degradation. A similar situation was also reported by Rodrigues et al. (2020) by comparing the distribution of Cd and Zn in surface sediments from periods 1990–2000 and 2000–2010, and by Molisani et al. (2004) and Araújo et al. (2017a) in sediment cores.

Benthic foraminifera are confirmed to be a resilient group of microorganisms and able to recover after severe stressful conditions (Bouchet et al., 2007; Oron et al., 2014) caused both by natural and anthropogenic processes. The biotic index $\exp(H'_{bc})$ applied on the fossil record appeared to be accurate in reflecting the environmental conditions occurring in the bay, confirming previous findings (see review in O'Brien et al., 2021). This index further complements the assessment of the environmental quality obtained from the chemical composition of the sediment. Direct (i.e., PTEs) and indirect (i.e., benthic foraminifera) indicators gave a complementary evaluation of the ecological quality. The former helps in identifying and quantifying the source of pollution, and the latter further illustrates the adverse effects of PTEs on living organisms. The results of this study also shed light on the potential of fossil foraminifera to serve as proxies for identification of *in situ* reference conditions (Alve et al., 2009; Dolven et al., 2013; Polovodova Asteman et al., 2021). Identification of local reference is crucial to reliably monitor the health of marine and transitional waters.

CONCLUSION

Core SP5 unveils the complex recent evolution of the Sepatiba Bay (SB) possibly associated with geomorphological and physiographical changes in the Guandu River delta. Between ≈1858 and1925, the study area did not present natural conditions favorable for foraminiferal settlement, as it was part of the adjacent coastal plain under riverine influence. With the retreat of the coastline and the establishment of an oceanic circulation from ≈1935, the environmental conditions became progressively more suitable for the establishment of benthic foraminiferal associations. From 1970 onward, the area became moderately to heavily polluted by PTEs mainly because of the urban and industrial development surrounding this region. In conjunction to metal contamination, the inner area of the SB has experienced a process of silting and eutrophication because of anthropic activities that conditioned the establishment of diversified assemblages of foraminifera. Opportunistic species (such as *A. tepida, B. elegantissima, B. striatula*, and *C. excavatum*) populated the area attracted by the abundant supply of organic matter. The foraminiferal-based biotic index $\exp(H'_{bc})$ has allowed us to reconstruct for the first time the PaleoEcoQS in the SB. The ecological conditions in the study area were poor around 1975 and worsened after the metal spill event from CIA Ingá tailings. However, the PaleoEcoQS became good in 2015, testifying an ongoing recovering phase. The SB is an invaluable environment from social, economic, and ecological points of view. Monitoring of this area is of great importance to take preventive actions and mitigate the environmental degradation of this system. This study shows that foraminiferal methods may be a very useful tool for the assessment of past environmental conditions and analysis of their temporal evolution.

DATA AVAILABILITY STATEMENT

The original contributions presented in the study are included in the article/**Supplementary Material**, further inquiries can be directed to the corresponding author/s.

AUTHOR CONTRIBUTIONS

LS, FFro, and TS-M contributed to formal analysis and writing (original draft). MVAM contributed to conceptualization, data curation, formal analysis, funding acquisition, investigation, methodology, project administration, resources, supervision, and writing (original draft). RF and EP contributed to data acquisition, formal analysis, and writing (original draft). WC, MS, FFra, VB, and LA contributed to writing (original draft). SM and SB contributed to investigation. DT contributed to formal analysis and data curation. FR contributed to resources. All authors contributed to the article and approved the submitted version.

ACKNOWLEDGMENTS

The authors would like to thank Conselho Nacional de Desenvolvimento Científico e Tecnológico of Brazil, CNPq (project processes # 443662/2018-5 and #302676/2019-8 to MVAM) and Fundação Carlos Chagas Filho de Amparo à Pesquisa do Estado do Rio de Janeiro, FAPERJ (project processes: E-26/202.927/2019 to MVAM) Brazil for financial support. The EP thanks CNPq and FAPERJ for the support to the LGQM. The authors would also like to thank Fundação para a Ciência e a Tecnologia – FCT, Portugal (GeoBioTec funding UID/GEO/04035/2019 and UIDB/04035/2020) for financial support. The authors would also like to thank Comitê Guandu–RJ for financially supporting the collection of the analyzed core, Professor Maria Antonieta Rodrigues for the transfer of the materials transfer, and Marcos Gonçalves of LGQM-UERJ for the technical support.

SUPPLEMENTARY MATERIAL

The Supplementary Material for this article can be found online at: https://www.frontiersin.org/articles/10.3389/fevo.2022.852439/full#supplementary-material

REFERENCES

Abadi, M., Zamani, A., Parizanganeh, A., Khosravi, Y., and Badiee, H. (2019). Distribution pattern and pollution status by analysis of selected heavy metal amounts in coastal sediments from the southern Caspian Sea. *Environ. Monit. Assess.* 191:144. doi: 10.1007/s10661-019-7261-2

Adelson, J. M., Helz, G. R., and Miller, C. V. (2001). Reconstructing the rise of recent coastal anoxia, molybdenum in Chesapeake Bay sediments. *Geochim. et Cosmochim. Acta* 65, 237–252. doi: 10.1016/s0016-7037(00)00539-1

Algeo, T. J., and Liu, J. (2020). A re-assessment of elemental proxies for paleoredox analysis. *Chem. Geol.* 540:119549. doi: 10.1016/j.chemgeo.2020.119549

Alve, E. (1995). Benthic foraminiferal distribution and recolonization of formerly anoxic environments in Drammensfjord, southern Norway. *Mar. Micropaleontol.* 25, 169–186. doi: 10.1016/0377-8398(95)00007-N

Alve, E., and Murray, J. W. (1999). Marginal marine environments of the Skagerrak and Kattegat: a baseline study of living (stained) benthic foraminiferal ecology. *Paleogeograph. Paleoclimatol. Paleoecol.* 146, 171–193. doi: 10.1016/s0031-0182(98)00131-x

Alve, E., Korsun, S., Schönfeld, J., Dijkstra, N., Golikova, E., Hess, C., et al. (2016). Foram-AMBI: a sensitivity index based on benthic foraminiferal faunas from North-East Atlantic and Arctic fjords, continental shelves and slopes. *Mar. Micropaleontol.* 122, 1–12. doi: 10.1016/j.marmicro.2015.11.001

Alve, E., Lepland, A., Magnusson, J., and Backer-Owe, K. (2009). Monitoring strategies for re-establishment of ecological reference conditions: Possibilities and limitations. *Mar. Pollut. Bull.* 59, 297–310. doi: 10.1016/j.marpolbul.2009.08.011

Alves Martins, M. V., Hohenegger, J., Frontalini, F., Sequeira, C., Miranda, P., Rodrigues, M. A. C., et al. (2019a). Foraminifera check list and the main species distribution in the Aveiro Lagoon and Adjacent Continental Shelf (Portugal). *J. Sediment. Environ.* 4, 1–52. doi: 10.12957/jse.2019.39308

Alves Martins, M. V., Pereira, E., Figueira, R. C. L., Oliveira, T., Pinto Simon, A. F. S., Terroso, D., et al. (2019b). Impact of eutrophication on benthic foraminifera in Sepetiba Bay (Rio de Janeiro State, SE Brazil). *J. Sediment.Environ.* 4, 480–500. doi: 10.12957/jse.2019.47327

Alves Martins, M. V., Hohenegger, J., Martínez-Colón, M., Frontalini, F., Bergamashi, S., Laut, L., et al. (2020). Ecological quality status of the NE sector of the Guanabara Bay (Brazil): a case of living benthic foraminiferal resilience. *Marin. Pollut. Bull.* 158, 111–449. doi: 10.1016/j.marpolbul.2020.111449

Alzieu, C. (2000). Impact of Tributyltin on Marine Invertebrates. *Ecotoxicology* 9, 71–76.

Amado-Filho, G. M., Andrade, L. R., Karez, C. S., Farina, M., and Pfeiffer, W. C. (1999). Brown algae species as biomonitors of Zn and Cd at Sepetiba Bay, Rio de Janeiro, Brazil. *Marin. Environ. Res.* 48, 213–224. doi: 10.1016/s0141-1136(99)00042-2

Araripe, D. R., Bellido, A. V. B., Patchineelam, S. R., Latini, R. M., Bellido, L. F., and Fávaro, D. I. T. (2011). Trace and major elements in geological samples from Itingusssú River Basin, Sepetiba Bay-Rio de Janeiro. *J. Radioanal. Nuclear Chem.* 290, 381–389. doi: 10.1007/s10967-011-1220-x

Araújo, D. F., Boaventura, G. R., Machado, W., Viers, J., Weiss, D., Patchineelam, S. R., et al. (2017b). Tracing of anthropogenic zinc sources in coastal environments using stable isotope composition. *Chem. Geol.* 449, 226–235. doi: 10.1016/j.chemgeo.2016.12.004

Araújo, D. F., Peres, L. G. M., Yepez, S., Mulholland, D. S., Machado, W., Tonhá, M., et al. (2017a). Assessing man-induced environmental changes in the Sepetiba Bay (Southeastern Brazil) with geochemical and satellite data. *Comptes. Rendus. Geosci.* 349, 290–298. doi: 10.1016/j.crte.2017.09.007

Araújo, F. G., de Azevedo, M. C. C., de Araújo Silva, M., Pessanha, A. L. M., Gomes, I. D., and Da Cruz-Filho, A. G. (2002). Environmental influences on the demersal fish assemblages in the Sepetiba Bay. *Brazil. Estuaries* 25, 441–450. doi: 10.1007/BF02695986

Asfers, Y., Taouil, H., Hafi, H., Elanza, S., Ibn Ahmed, S., and Aboulouafa, M. (2017). Study of the Sediments Metallic Contamination in Oum Er-Rbia Estuary. *IOSR J. Appl. Chem.* 10, 67–75. doi: 10.1016/j.scitotenv.2014.12.098

Azevedo, S. V., Sobral, A., and Moreira, M. F. R. (2019). Spatial pattern of the environmental exposure to tin in the vicinity of an alloy industry in Volta Redonda, Rio de Janeiro State, Brazil. *Cad. Saúde Pública* 35:e00079818. doi: 10.1590/0102-311X00079818

Balkıs, N., Topçuoğlu, S., Güven, K. C., Öztürk, B., Topaloğlu, B., Kırbaşoğlu, Ç, et al. (2007). Heavy metals in shallow sediments from the Black Sea, Marmara Sea and Aegean Sea regions of Turkey. *J. Black Sea/Mediterranean Environ.* 13, 147–153.

Barbosa, C. (2005). Foraminiferal zonations as base lines for Quaternary sea-level fluctuations in south-southeast Brazilian mangroves and marshes. *J. Foraminiferal Res.* 35, 22–43. doi: 10.2113/35.1.22

Barcellos, C., Lacerda, L. D., and Ceradini, S. (1997). Sediment origin and budget in Sepetiba Bay (Brazil) - An approach based on multi-element analysis. *Environ. Geol.* 32, 203–209. doi: 10.1007/s002540050208

Barcellos, C., Pedlowski, M. A., Rezende, C. E., Pfeiffer, W. C., and Lacerda, L. D. (1991). Sources and sinks of lead in Sepetiba Bay. In: CEP Consultants. *Heavy Metals Environ.* 1, 535–538.

Barras, C., Jorissen, F. J., Labrune, C., Andral, B., and Boissery, P. (2014). Live benthic foraminiferal faunas from the French Mediterranean coast: towards a new biotic index of environmental quality. *Ecol. Indic.* 36, 719–743. doi: 10.1016/j.ecolind.2013.09.028

Barros, G. V., Martinelli, L. A., Oliveira Novais, T. M., Ometto, J. P., and Zuppi, G. M. (2010). Stable isotopes of bulk organic matter to trace carbon and nitrogen dynamics in an estuarine ecosystem in Babitonga Bay (Santa Catarina, Brazil). *Sci. Total Environ.* 408, 2226–2232. doi: 10.1016/j.scitotenv.2010.01.060

Bhatia, M. R., and Crook, K. A. (1986). Trace element characteristics of graywackes and tectonic setting discrimination of sedimentary basins. *Contribut. Mineral. Petrol.* 92, 181–193. doi: 10.1007/bf00375292

Blanchet, H., Lavesque, N., Ruellet, T., Dauvin, J.-C., Sauriau, P. G., Desroy, N., et al. (2008). Use of biotic indices in semi-enclosed coastal ecosystems and transitional waters habitats - implications for the implementation of the European water framework directive. *Ecol. Indic.* 8, 360–372. doi: 10.1016/j.ecolind.2007.04.003

Blott, S. J., and Pye, K. (2001). Gradistat: A Grain Size Distribution and Statistics Package for the Analysis of Unconsolidated Sediments. *Earth Surface Process. Landforms* 26, 1237–1248. doi: 10.1002/esp.261

Boltovskoy, E., Giussani, G., Watanabe, S., and Wright, R. (1980). *Atlas of Benthic Shelf Foraminifera of Southwest Atlantic*. The Hague: Dr W Junk bv Publishers.

Borges, H. V., and Nittrouer, C. A. (2016a). Coastal Sedimentation in a Tropical Barrier-Island System During the Past Century in Sepetiba Bay, Brazil. *Anuário do Instituto de Geociências – UFRJ* 39, 5–14. doi: 10.11137/2016_2_05_14

Borges, H. V., and Nittrouer, C. A. (2016b). Sediment accumulation in Sepetiba Bay (Brazil) during the Holocene: A reflex of the human influence. *J. Sediment. Environ.* 1, 96–112. doi: 10.12957/jse.2016.21868

Bouchet, V. M. P., Debenay, J.-P., Sauriau, P.-G., Radford-Knoery, J., and Soletchnik, P. (2007). Effects of short-term environmental disturbances on living benthic foraminifera during the Pacific oyster summer mortality in the Marennes-Oléron Bay (France). *Mar. Environ. Res.* 64, 358–383. doi: 10.1016/j.marenvres.2007.02.007

Bouchet, V. M. P., Deldicq, N., Baux, N., Dauvin, J.-C., Pezy, J.-P., Seuront, L., et al. (2020). Benthic foraminifera to assess ecological quality status: the case of salmon fish farming. *Ecol. Indic.* 117:106607. doi: 10.1016/j.ecolind.2020.106607

Bouchet, V. M. P., Frontalini, F., Francescangeli, F., Sauriau, P.-G., Geslin, E., Martins, M. V. A., et al. (2021). Indicative value of benthic foraminifera for biomonitoring: assignment to ecological groups of sensitivity to total organic carbon of species from European intertidal areas and transitional waters. *Marin. Pollut. Bull.* 164:112071. doi: 10.1016/j.marpolbul.2021.112071

Bouchet, V. M. P., Goberville, E., and Frontalini, F. (2018a). Foraminifera to assess ecological quality status: the case of salmon fish farming. *Ecol. Indic* 117:106607. ecolind.2020.106607 doi: 10.1016/j

Bouchet, V. M. P., Goberville, E., and Frontalini, F. (2018b). Benthic foraminifera to assess Ecological Quality Status in Italian transitional waters. *Ecol. Indic.* 84, 130–139. doi: 10.1016/j.ecolind.2017.07.055

Bouchet, V. M., Alve, E., Rygg, B., and Telford, R. J. (2012). Benthic foraminifera provide a promising tool for ecological quality assessment of marine waters. *Ecol. Indic.* 23, 66–75. doi: 10.1016/j.ecolind.2012.03.011

Brönnimann, P., Moura, J. A., and Dias-Brito, D. (1981). *Ecologia dos foraminíferos e microrganismos associados da área de Guaratiba/Sepetiba: Modelo ambiental e sua aplicação na pesquisa de hidrocarbonetos*. (Rio de Janeiro: Petrobras).

Brown, E. T., Le Callonnec, L., and German, C. R. (2000). Geochemical cycling of redox-sensitive metals in sediments from Lake Malawi: a diagnostic paleotracer for episodic changes in mixing depth. *Geochim. et Cosmochim. Acta* 64, 3515–3523. doi: 10.1016/s0016-7037(00)00460-9

Buat-Menard, P., and Chesselet, R. (1979). Variable influence of the atmospheric flux on the trace metal chemistry of oceanic suspended matter. *Earth Planet. Sci. Lett.* 42, 398–411. doi: 10.1016/j.marpolbul.2014.12.030

Bueno, C., Figueira, R., Ivanoff, M. D., Toldo Junior, E. E., Fornaro, L., and García-Rodríguez, F. G. (2019). A multi proxy assessment of long-term anthropogenic impacts in Patos Lagoon, southern Brazil. *J. Sediment. Environ.* 4, 276–290. doi: 10.12957/jse.2019.44612

Campbell, F. A., and Williams, G. D. (1965). Chemical composition of shales of Mannville group (lower Cretaceous) of central Alberta, Canada. *Am. Assoc. Pet. Geol. Bull.* 49, 81–87.

Carneiro, C. S., Mársico, E. T., Ribeiro, R. O. R., and Jesus, E. F. O. (2013). Total Mercury Bioaccumulation in Tissues of Carnivorous Fish (Micropogonias furnieriandCynoscion acoupa) and Oysters (Crassostrea brasiliana) from Sepetiba Bay, Brazil. *J. Aquatic Food Product Technol.* 22, 96–102. doi: 10.1080/10498850.2011.627007

Castelo, W. F. L., Alves Martins, M. V., Ferreira, P. A. L., Figueira, R., Costa, C. F., Fonseca, L. B., et al. (2021b). Long-term eutrophication and contamination of the central area of Sepetiba Bay SW Brazil. *Environ. Monitor. Assess.* 193:100. doi: 10.1007/s10661-021-08861-1

Castelo, W. F. L., Alves Martins, M. V., Martínez-Colón, M., Guerra, J. V., Dadalto, T. P., Terroso, D., et al. (2021a). Disentangling natural vs. anthropogenic induced environmental variability during the Holocene: Marambaia Cove, SE sector of the Sepetiba Bay SE Brazil. *Environ. Sci.Pollut. Res.* 28, 22612–22640. doi: 10.1007/s11356-020-12179-9

Copeland, G., Monteiro, T., Couchc, S., and Borthwick, A. (2003). Water quality in Sepetiba Bay, Brazil. *Marin. Environ. Res.* 55, 385–408. doi: 10.1016/S0141-1136(02)00289-1

Cullers, R. L. (2002). Implications of elemental concentrations for provenance, redox conditions, and metamorphic studies of shales and limestones near Pueblo, CO, USA. *Chem. Geol.* 191, 305–327. doi: 10.1016/s0009-2541(02)00133-x

Cunha, C. L. N., Rosman, P. C. C., Ferreira, A. F., and Monteiro, T. C. N. (2006). Hydrodynamics and water quality models applied to Sepetiba Bay. *Continent. Shelf Res. Arch.* 26, 1940–1953. doi: 10.1016/j.csr.2006.06.010

Debenay, J. P., Geslin, E., Eichler, B. B., Duleba, W., Sylvestre, F., and Eichler, P. (2001). Foraminifera assemblages in a hypersaline lagoon: the Lagoon of Araruama (RJ), Brazil. *J. Foraminiferal Res.* 31, 133–155. doi: 10.2113/0310133

Deines, P. (1980). "The isotopic composition of reduced organic carbon," in *Handbook of Environmental Isotope Geochemistry*, eds P. Fritz and J. C. H. Fontes (Amsterdam: Elsevier Scientific Publishing Company), 1, 329–406. doi: 10.1016/b978-0-444-41780-0.50015-8

Díaz Morales, S. J., Guerra, J. V., Nunes, M. A. S., Souza, A. M., and Geraldes, M. C. (2019). Evaluation of the environmental state of the western sector of Sepetiba Bay (SE Brazil): trace metal contamination. *J. Sediment. Environ.* 4, 174–188. doi: 10.12957/jse.2019.43764

Dolven, J. K., Alve, E., Rygg, B., and Magnusson, J. (2013). Defining past ecological status and in situ reference conditions using benthic foraminifera: A case study from the Oslofjord, Norway. *Ecol. Indic.* 29, 219–233. doi: 10.1016/j.ecolind.2012.12.031

Dourado, F., Cunha, J., Lima, A., and Palermo, N. (2012). "Os novos Empreendimentos na Baía de Sepetiba e o Passivo Ambiental da Cia Mercantil e Industrial Ingá". In *Baía de Sepetiba: Estado da Arte*, eds Rodrigues, M. A. C., Pereira, S. D., Santos, S. B. (Rio de Janeiro: Editora Corbã)

Duleba, W. E., and Debenay, J. P. (2003). Hydrodynamic circulation in the estuaries of Estação Ecológica Jureia-Itatins, Brazil, inferred from foraminifera and thecamoebian assemblages. *J. Foraminiferal Res.* 33, 62–93. doi: 10.2113/0330062

Duleba, W., Gubitoso, S., Alves Martins, M. V., Teodoro, A. C., Pregnolato, L. A., and Prada, S. M. (2019). Evaluation of Contamination by Potentially Toxic Elements (PTE) of Sediments around the Petroleum Terminal Pipeline "Dutos e Terminais do Centro Sul (DTCS)", SP, Brazil. *J. Sediment. Environ.* 4, 387–402. doi: 10.12957/jse.2019.46539

Duleba, W., Teodoro, A. C., Debenay, J.-P., Alves Martins, M. V., Gubitoso, S., Pregnolato, L. A., et al. (2018). Environmental impact of the largest petroleum terminal in SE Brazil: A multiproxy analysis based on sediment geochemistry and living benthic foraminifera. *PLoS One* 13:e0191446. doi: 10.1371/journal.pone.0191446

Elliott, M., and Quintino, V. (2007). The Estuarine Quality Paradox, environmental homeostasis and the difficulty of detecting anthropogenic stress in naturally stressed areas. *Mar. Pollut. Bull.* 54, 640–645. doi: 10.1016/j.marpolbul.2007.02.003

Ellis, B. F., Messina, A. (1940-2015) *Catalogue of Foraminifera*. (New York, NY: Micropaleontology Press, American Museum of Natural History).

Fatela, F., and Taborda, R. (2002). Confidence limits of species proportions in microfossil assemblages. *Marin. Micropaleontol.* 45, 169–174. doi: 10.1016/s0377-8398(02)00021-x

Ferreira, A. P., and Moreira, M. D. F. R. (2015). Metals pollution status in surface sediments along the Sepetiba Bay Watershed, Brazil. *J. Coast. Zone Manage.* 18:404. doi: 10.4172/2473-3350.1000404

Ferreira, P. A. L., Siegle, E., Schettini, C. A. F., de Mahiques, M. M., and Figueira, R. C. L. (2014). Statistical validation of the model of diffusion-convection MDC of 137Cs for the assessment of recent sedimentation rates in coastal systems. *J. Radioanal. Nuclear Chem.* 1, 1–13. doi: 10.1007/s10967-014-3622-z

Figueira, R. C. L., Tessler, M. G., Mahiques, M. M., and Fukumoto, M. M. (2007). Is there a technique for the determination of sedimentation rates based on calcium carbonate content? A comparative study on the Southeastern Brazilian shelf. *Soils Found.* 47, 649–656. doi: 10.3208/sandf.47.649

Folk, R. L., and Ward, W. C. (1957). Brazos River bar: a study in the significance of grain size parameters. *J. Sediment. Petrol.* 27, 3–26. doi: 10.1306/74d70646-2b21-11d7-8648000102c1865d

Francescangeli, F., Armynot, du Chatelet, E., Billon, G., Trentesaux, A., and Bouchet, V. M. (2016). PalaeoPaleo-ecological quality status based on foraminifera of Boulogne-sur-Mer harbour (Pas-de-Calais, Northeastern France) over the last 200 years. *Mar Environ Res.* 117, 32–43. doi: 10.1016/j.marenvres.2016.04.002

Francescangeli, F., Portela, M., Armynot, du Chatelet, E., Billon, G., Andersen, T. J., et al. (2018). Infilling of the Canche Estuary (eastern English Channel, France): Insight from benthic foraminifera and historical pictures. *Marin. Micropaleontol.* 142, 1–12. doi: 10.1016/j.marmicro.2018.05.003

Francescangeli, F., Quijada, M., Armynot, du Châtelet, E., Frontalini, F., Trentesaux, A., et al. (2020). Multidisciplinary study to monitor consequences of pollution on intertidal benthic ecosystems (Hauts de France, English Channel, France): comparison with natural areas. Mar. *Environ. Res.* 160:105034. doi: 10.1016/j.marenvres.2020.105034

Freret-Meurer, N. V., Andreata, J. V., Meurer, B. C., Manzano, F. V., Baptista, M. G. S., Teixeira, D. E., et al. (2010). Spatial distribution of metals in sediments of the Ribeira Bay, Angra dos Reis, Rio de Janeiro, Brazil. *Marin. Pollut. Bull.* 60, 627–629. doi: 10.1016/j.marpolbul.2010.01.023

Friederichs, Y. L., Reis, A. T., Silva, C. G., Toulemonde, B., Maia, R. M. C., and Guerra, J. V. (2013). The seismic architecture of the Sepetiba fluvio-estuarine system preserved on the shallow stratigraphic record on the offshore inner-mid shelf, Rio de Janeiro, Brazil. *Brazil. J. Geol.* 43, 124–138. doi: 10.5327/Z2317-48892013000100011

Frontalini, F., Buosi, C., Da Pelo, S., Coccioni, R., Cherchi, A., and Bucci, C. (2009). Benthic foraminifera as bio-indicators of trace element pollution in the heavily contamined Santa Gilla lagoon (Cagliari, Italy). *Marin. Pollut. Bull.* 58, 858–877. doi: 10.1016/j.marpolbul.2009.01.015

Fundação Estadual de Engenharia do Meio Ambiente [FEEMA] (1997). *Mapeamento de sedimentos da Baía de Sepetiba. Contaminação por metais pesados. Relatório Técnico Abril/97*. (Washington, DC: FEEMA).

Gao, X., and Chen, C. T. A. (2012). Heavy metal pollution status in surface sediments of the coastal Bohai Bay. *Water Res.* 46, 1901–1911. doi: 10.1016/j.watres.2012.01.007

Garver, J. I., Royce, P. R., and Smick, T. A. (1996). Chromium and nickel in shale of the Taconic foreland, a case study for the provenance of fine–grained sediments with an ultramafic source. *J. Sediment. Res.* 66, 100–106.

Gebregiorgis, D., Giosan, L., Hathorne, E. C., Anand, P., Nilsson-Kerr, K., and Plass, A. (2020). What can we learn from X-ray fluorescence core scanning data? A paleomonsoon case study. *Geochem. Geophys. Geosyst.* 21:e2019GC008414. doi: 10.1029/2019GC008414

Gonçalves, R. A., Oliveira, D. F., Rezende, C. E., Almeida, P., de Lacerda, L. D., Gama, B. A. P., et al. (2020). Spatial and temporal effects of decommissioning a zinc smelter on the sediment quality of an estuary system: Sepetiba Bay, Rio de Janeiro, Brazil. *J. Braz. Chem. Soc.* 31, 683–693. doi: 10.21577/0103-5053.20190232

Håkanson, L. (1980). Ecological risk index for aquatic pollution control. A sedimentological approach. *Water Res.* 14, 975–1001. doi: 10.1016/0043-1354(80)90143-8

Hausser, J., and Strimmer, K. (2014). *Entropy: Estimation of Entropy, Mutual Information and Related Quantities. R package version*. (Vienna, Austria: R foundation for statistical computing).

Hayward, B.-W., Le Coze, F., Vandepitte, L., and Vanhoorne, B. (2020). Foraminifera in the World Register of Marine Species (Worms) Taxonomic Database. *J. Foraminiferal Res.* 50, 291–300. doi: 10.2113/gsjfr.50.3.291

Heilbron, M., Silva, L. G. E., Almeida, J. C. H., Tupinambá, M., Peixoto, C., Valeriano, C. M., et al. (2020). Proterozoic to Ordovician geology and tectonic evolution of Rio de Janeiro State, SE-Brazil: insights on the central Ribeira Orogen from the new 1:400,000 scale geologic map. *Brazil. J. Geol.* 50, 1–25. doi: 10.1590/2317-4889202020190099

Hess, S., Alve, E., Andersen, T. J., and Joranger, T. (2020). Defining ecological reference conditions in naturally stressed environments – how difficult is it? *Mar. Environ. Res.* 156:104885. doi: 10.1016/j.marenvres.2020.104885

Hiscott, R. (1984). Ophiolitic source rocks for Taconic-age flysch: trace element evidence. *Geol. Soc. Am. Bull.* 95, 1261–1267. doi: 10.1130/0016-7606(1984)95<1261:osrftf>2.0.co;2

Hossain, H. Z., Kawahata, H., Roser, B. P., Sampei, Y., Manaka, T., and Otani, S. (2017). Geochemical characteristics of modern river sediments in Myanmar and Thailand: implications for provenance and weathering. *Geochemistry* 77, 443–458. doi: 10.1016/j.chemer.2017.07.005

Hwang, H. M., Green, P. G., Higashi, R. M., and Young, T. M. (2006). Tidal salt marsh sediment in California, USA. Part 2: occurrence and anthropogenic input of trace metals. *Chemosphere* 64, 1899–1909. doi: 10.1016/j.chemosphere.2006.01.053

Jesus, M. S. D. S., Frontalini, F., Bouchet, V. M. P., Yamashita, C., Sartoretto, J. R., Figueira, R. C. L., et al. (2020). Reconstruction of the palaeopaleo-ecological quality status in an anthropogenised estuary using benthic foraminifera: the Santos estuary (Sao Paulo state, SE Brazil). *Mar. Env. Res.* 162:105121. doi: 10.1016/j.marenvres.2020.105121

Jesus, W. B., Andrade, T. S. O. M., Sores, S. H., Pinheiro-Sousa, D. B., Oliveira, S. R. S., Torres, H. S., et al. (2021). Biomarkers and occurrences of heavy metals in sediment and the bioaccumulation of metals in crabs (Ucides cordatus) in impacted mangroves on the Amazon coast, Brazil. *Chemosphere* 271:129444. doi: 10.1016/j.chemosphere.2020.129444

Kato, K., and Quintela, S. (2012). *Companhia siderúrgica do atlântico: impactos e irregularidades na Zona Oeste do Rio de Janeiro*. (Rio de Janeiro: Publicaçao PACS.)

Kennish, M. J. (1997). *Estuarine and Marine Pollution, Practical Handbook*. (Florida: CRC Press), 524.

Kjerfve, B., Dias, G. T. M., Filippo, A. F., and Geraldes, M. C. (2021). Oceanographic and environmental characteristics of a coupled coastal bay system: Baía de Ilha Grande-Baía de Sepetiba, Rio de Janeiro, Brazil. *Region. Stud. Marin. Sci.* 41:101594. doi: 10.1016/j.rsma.2020.101594

Kottek, M., Grieser, J., Beck, C., Rudolf, B., and Rubel, F. (2006). World Map of the Köppen-Geiger climate classification updated. *Meteorol. Z.* 15, 259–263. doi: 10.1127/0941-2948/2006/0130

Lacerda, L. D., and Molisani, M. M. (2006). Three decades of Cd and Zn contamination in Sepetiba Bay, SE Brazil: Evidence from the mangrove oyster *Crassostrea rhizophorae*. *Marin. Pollut. Bull.* 52, 969–987. doi: 10.1016/j.marpolbul.2006.04.007

Lacerda, L. D., Marins, R. V., Barcellos, C., and Molisani, M. M. (2004). "Sepetiba Bay: A Case Study of the Environmental Geochemistry of Heavy Metals in a Subtropical Coastal Lagoon". in *Environmental Geochemistry in Tropical and Subtropical Environments*, eds Lacerda, L.D., Santelli, R.E., Abra o, J.J., Duursma, E.K (Berlin: SpringerVerlag), 293–318. doi: 10.1007/978-3-662-07060-4_21

Lacerda, L. D., Marins, R. V., Paraquetti, H. H. M., Mounier, S., Benaim, J., and Fevrier, D. (2001). Mercury distribution and reactivity in waters of a subtropical coastal lagoon, Sepetiba Bay, SE Brazil. *J. Brazil. Chem. Soc.* 12, 93–98.

Lacerda, L. D., Pfeiffer, W. C., and Fiszman, M. (1987). Heavy metal distribution, availability and fate in Sepetiba Bay, S.E. Brazil. *Sci. Total Environ.* 65, 163–173. doi: 10.1016/0048-9697(87)90169-0

Lamb, A. L., Wilson, G. P., and Leng, M. J. (2006). A review of coastal palaeopaleoclimate and relative sea-level reconstructions using $\delta^{13}C$ and C/N ratios in organic material. *Earth Sci. Rev.* 75, 29–57. doi: 10.1016/j.earscirev.2005.10.003

Lira, H. L., and Neves, G. A. (2013). Feldspatos: conceitos, estrutura cristalina, propriedades físicas, origem e ocorrências, aplicações, reservas e produção. *Revista Eletrônica de Materiais e Processos* 8, 110–117.

Liu, X., Zhang, M., Li, A., Fan, D., Dong, J., Jiao, C., et al. (2021). Depositional control on carbon and sulfur preservation onshore and offshore the Oujiang Estuary: Implications for the C/S ratio as a salinity indicator. *Continental Shelf Res.* 227:104510. doi: 10.1016/j.csr.2021.104510

Liu, Y. J., and Cao, L. M. (1984). *Element Geochemistry*. (Beijing: Science Press), 72–110.

Loeblich, A. R., and Tappan, H. (1987). *Foraminiferal Genera and their Classification*. (New York, NY: Van Nostrand Reinhold Company), 970.

Lyons, T. W., and Berner, R. A. (1992). Carbon-sulfur-iron systematics of the uppermost deep-water sediments of the Black Sea. *Chem. Geol.* 99, 1–27. doi: 10.1016/0009-2541(92)90028-4

Magalhães, V. F., and Pfeiffer, W. C. (1995). Arsenic concentration in sediments near a metallurgical plant (Sepetiba Bay, Rio de Janeiro, Brazil). *J. Geochem. Explor.* 52, 175–181. doi: 10.1016/0375-6742(94)00025-7

Magalhães, V. F., Carvalho, C. E. V., and Pfeiffer, W. C. (2001). Arsenic contamination and dispersion in the Engenho Inlet, Sepetiba Bay, SE, Brazil. *Water Air Soil Pollut.* 129, 83–90. doi: 10.1023/A:1010381902874

Marques, A. N. Jr., Monna, F., Silva-Filho, E. V., Fernex, F. E., and Simões Filho, F. F. L. (2006). Apparent discrepancy in contamination history of a sub-tropical estuary evaluated through ^{210}Pb profile and chronostratigraphical markers. *Mar. Pollut. Bull.* 52, 532–539. doi: 10.1016/j.marpolbul.2005.09.048

Martinelli, L. P., Ometto, J. P. H. B., Ferraz, E. S., Victoria, R. L., Camargo, P. B., and Moreira, M. Z. (2009). *Desvendando Questões Ambientais com Isótopos Estáveis [Unraveling Environmental Issues with Stable Isotopes.]*. São Paulo: Oficina de Textos

Martins, M. V. A., and Gomes, V. C. R. D. (2004). *Foraminíferos da margem continental NW Ibérica: sistemática, ecologia e distribuição*, 1ª Edn. (Aveiro: Universidade de Aveiro).

Martins, M. V. A., Pereira, E., Figueira, R. C. L., Oliveira, T., Simon, A. F. S. P., Terroso, D., et al. (2019). Impact of eutrophication on benthic foraminifera in Sepetiba Bay (Rio de Janeiro State, SE Brazil). *J. Sediment. Environ.* 4, 480–500. doi: 10.12957/jse.2019.47327

Martins, M. V., Silva, F., Laut, L. L., Frontalini, F., Clemente, I. M., Miranda, P., Figueira, R., Sousa, S. H., et al. (2015). Response of benthic foraminifera to organic matter quantity and quality and bioavailable concentrations of metals in Aveiro Lagoon (Portugal). *PLoS One* 10:e0118077. doi: 10.1371/journal.pone.0118077

Martins, V., Dubert, J., Jouanneau, J.-M., Weber, O., Silva, E. F., Patinha, C., et al. (2007). A multiproxy approach of the Holocene evolution of shelf–slope circulation on the NW Iberian Continental Shelf. *Marin. Geol.* 239, 1–18. doi: 10.1016/j.margeo.2006.11.001

McCune, B., and Mefford, M. J. (2016). *PC-ORD. Multivariate Analysis of Ecological Data. Version 7*. (Gleneden Beach, Oregon: MjM Software Design)

Melo, L. M. (1996). *Comportamento de Poluentes Metálicos Dissolvidos nas Águas da Baía de Sepetiba.1996, 98p. Dissertação de Mestrado em Geociências - Geoquímica*. (Niterói: Instituto de Química, Universidade Federal Fluminense)

Meyers, P. A. (1997). Organic geochemical proxies of paleoceanographic, paleolimnologic and paleoclimatic processes. *Org. Geochem.* 27, 213–250. doi: 10.1016/s0146-6380(97)00049-1

Milligan, G., and Cooper, M. (1985). An examination of procedures for determining the number of clusters in a data set. *Psychometrika* 50, 159–179. doi: 10.1007/bf02294245

Mirlean, N., and Baisch, P. (2016). "Arsenic in Brazilian tropical coastal zone," in *Arsenic Research and Global Sustainability*, eds P. Bhattacharya, M. Vahter, J. Jarsjö, J. Kumpiene, A. Ahmad, C. Sparrenbom, et al. (London: Taylor & Francis Group), 169–170. doi: 10.1201/b20466-82

Molisani, M. M., Marins, R. V., Machado, W., Paraquetti, H. H. M., Bidone, E. D., and Lacerda, L. D. (2004). Environmental changes in Sepetiba Bay, SE Brazil. *Reg. Environ. Changes* 4, 17–27. doi: 10.1007/s10113-003-0060-9

Moodley, L., and Hess, C. (1992). Tolerance of infaunal benthic foraminifera for low and high oxygen concentrations. *Biol. Bull.* 183, 94–98. doi: 10.2307/1542410

Moreira, L. L. (2012). *Caracterização da contamição metálica e adequação da Sparti alterniflora como espécie bioindicadora de contamição no estuário da Lagoa pos Patos: base para a gestão ambiental do estuário*. [Ph.D thesis]. (Brazil: Universidade Federal do Rio Grande)

Mounier, S., Lacerda, L. D., Marins, R. V., and Benaim, J. (2001). Copper and Mercury Complexing Capacity of Organic Matter From a Mangrove Mud

Flat Environment, Sepetiba Bay, Brazil. *Bull. Environ. Contaminat. Toxicol.* 67, 519–525. doi: 10.1007/s001280154

Müller, V. G. (1986). Schadstoffe in Sedimenten - Sedimente als Schadstoffe. *Mitteilungen der Österreichischen Geologischen Gesellschaft* 79, 107–126.

Murray, J. (2006). *Ecology and Applications of Benthic Foraminifera*. New York, NY: Cambridge University Press, 426. Melbourne xi +.

Murray, J. W. (1991). *Ecology and Palaeopaleoecology of Benthic Foraminifera*. London: Longman Scientific and Technical, 397.

Nace, T. E., Baker, P. A., Dwyer, G. S., Silva, C. G., Rigsby, C. A., Burns, S. J., et al. (2014). The role of North Brazil Current transport in the paleoclimate of the Brazilian Nordeste margin and paleoceanography of the western tropical Atlantic during the late Quaternary. *Paleogeogr. Paleoclimatol. Paleoecol.* 415, 3–13. doi: 10.1016/j.palaeopaleo.2014.05.030

Nordstrom, D. K., and Archer, D. G. (2003). "Chapter 1 – Arsenic thermodynamic data and environmental geochemistry," in *Arsenic in Ground Water*, ed. A. H. Welch and K. G. Stollenwerk (Boston, MA: Kluwer Academic Publishers). doi: 10.1007/0-306-47956-7_1

NORMAM-23/DPC (2007). *Normas da Autoridade Marítima Para o Controle de Sistemas Antiincrustantes Danosos em Embarcações*. (Brasil: Marinha do Brasil).

O'Brien, P., Polovodova Asteman, I., and Bouchet, V. M. P. (2021). Benthic foraminiferal indices and environmental quality assessment of transitional waters: a review of current challenges and future research perspectives. *Water* 13:1898. doi: 10.3390/w13141898

O'Day, P. A. (2006). Chemistry and mineralogy of arsenic. *Elements*, 2, 77–83. doi: 10.2113/gselements.2.2.77

Okunlola, O. A., and Idowu, O. (2012). The geochemistry of claystone-shale deposits from the Maastritchian Patti formation, Southern Bida basin, Nigeria. *Earth Sci. Res. J.* 16, 139–150.

Oron, S., Angel, D., Goodman-Tchernov, B., Merkado, G., Kiflawi, M., and Abramovich, S. (2014). Benthic foraminiferal response to the removal of aquaculture fish cages in the Gulf of Aqaba-Eilat, Red Sea. *Marin. Micropaleontol.* 107, 8–17. doi: 10.1016/j.marmicro.2014.01.003

Paraquetti, H. H. M., Ayres, G. A., Almeida, M. D., Molisani, M. M., and Lacerda, L. D. (2004). Mercury distribution, speciation and flux in the Sepetiba Bay tributaries, SE Brazil. *Water Res.* 38, 1439–1448. doi: 10.1016/j.watres.2003.11.039

Peel, M. C., Finlayson, B. L., and Mcmahon, T. A. (2007). Updated world map of the Köppen-Geiger climate classification. – Hydrol. *Earth Syst. Sci.* 11, 1633–1644. doi: 10.5194/hess-11-1633-2007

Pekey, H. (2006). The distribution and sources of heavy metals in Izmit Bay surface sediments affected by a polluted stream. *Marin. Pollut. Bull.* 52, 1197–1208. doi: 10.1016/j.marpolbul.2006.02.012

Pellegatti, F., Figueiredo, A. M. G., and Wasserman, J. C. (2001). Neutron Activation Analysis Applied to the Determination of Heavy Metals and Other Trace Elements in Sediments from Sepetiba Bay (RJ), Brazil. *Geostand. Newslett.* 25, 307–315. doi: 10.1111/j.1751-908X.2001.tb00607.x

Pereira, R. M., Ávila, C. A., and Neumann, R. (2003). Prospecção para cassiterita na região entre Cachoeira Paulista (SP) e Resende (RJ): potencialidade em estanho dos granitos do funil e São José do Barreiro, segmento central da Faixa Ribeira. *São Paulo* 22, 107–119.

Perillo, G. M. E. (1995). Chapter 1 Geomorphology and Sedimentology of Estuaries: An Introduction. *Geomorphol. Sedimentol. Estuaries* 53, 1–16. doi: 10.1016/s0070-4571(05)80021-4

Pinto, A. F. S., Ramalho, J. C. M., Borghi, L., Carelli, T. G., Plantz, J. B., Pereira, E., et al. (2019). Background concentrations of chemical elements in Sepetiba Bay (SE Brazil). *J. Sediment. Environ.* 4, 108–123. doi: 10.12957/jse.2019.40992

Polovodova Asteman, I., Van Nieuwenhove, N., Andersen, T. J., Linders, T., and Nordberg, K. (2021). Recent environmental change in the Kosterhavet National Park marine protected area as reflected by hydrography and sediment proxy data. *Mar. Environ. Res.* 166:105265. doi: 10.1016/j.marenvres.2021.105265

Prazeres, M., Uthicke, S., and Pandolfi, J. M. (2015). Ocean acidification induces biochemical and morphological changes in the calcification process of large benthic foraminifera. *Proc. R. Soc. B* 282:20142782. doi: 10.1098/rspb.2014.2782

Protano, C., Zinnà, L., Giampaoli, S., Romano Spica, V., Chiavarini, S., and Vitali, M. (2014). Heavy Metal Pollution and Potential Ecological Risks in Rivers: A Case Study from Southern Italy. *Bull. Environ. Contaminat. Toxicol.* 92, 75–80. doi: 10.1007/s00128-013-1150-0

Quaresma, V. S., Aguiar, V. M. C., Bastos, A. C., Oliveira, K. S., Vieira, F. V., Sá, F., et al. (2021). The impact of trace metals in marine sediments after a tailing dam failure: the Fundão dam case (Brazil). *Environ. Earth Sci.* 80:571. doi: 10.1007/s12665-021-09817-x

R Core Team (2016). *R: A Language and Environment for Statistical Computing*. Vienna, Austria: R foundation for statistical computing.

Reimann, C., Matschullat, J., Birke, M., and Salminen, R. (2009). Arsenic distribution in the environment: the effects of scale. *Appl. Geochem.* 24, 1147–1167. doi: 10.1016/j.apgeochem.2009.03.013

Reis, A. T., Amendola, G., Dadalto, T. P., Silva, C. G., Tardin Poço, R., Guerra, J. V., et al. (2020). Arquitetura e evolução deposicional da sucessão sedimentar pleistoceno tardio-holoceno (últimos ˜20 ka) da Baía de Sepetiba (RJ). *Revista Brasileira de Geociências* 39, 695–708. doi: 10.5016/geociencias.v39i03.14366

Ribeiro, A. P., Figueiredo, A. M., dos Santos, J. O., Dantas, E., Cotrim, M. E., Figueira, R. C., et al. (2013). Combined SEM/AVS and attenuation of concentration models for the assessment of bioavailability and mobility of metals in sediments of Sepetiba Bay (SE Brazil). *Marin. Pollut. Bull.* 15, 55–63. doi: 10.1016/j.marpolbul.2012.12.023

Rodrigues, S. K., Machado, W., Guerra, J. V., Geraldes, M., Morales, S., and Vinzóna, S. B. (2020). Changes in Cd and Zn distribution in sediments after closure of an electroplating industry, Sepetiba bay, Brazil. *Marin. Pollut. Bull.* 161:111758. doi: 10.1016/j.marpolbul.2020.111758

Rogers, E. J. (1968). Brazilian Success Story: The Volta Redonda Iron and Steel Project. *J. Inter Am. Stud.* 10, 637–652. doi: 10.2307/165321

Roncarati, H., and Carelli, S. G. (2012). "Considerações sobre o estado da arte dos processos geológicos cenozóicos atuantes na Baía de Sepetiba," in *Baía de Sepetiba: Estado da Arte*, eds M. A. C. Rodrigues, S. D. Pereira, and S. B. Santos (Rio de Janeiro: Corbã), 13–36.

Salas, P. M., Sujatha, C. H., Kumar, C. S. R., and Cheriyan, E. (2017). Heavy metal distribution and contamination status in the sedimentary environment of Cochin estuary. *Marin. Pollut. Bull.* 119, 191–203. doi: 10.1016/j.marpolbul.2017.04.018

Santos Bermejo, J., Beltrán, R., and Gómez Ariza, J. (2003). Spatial variations of heavy metals contamination in sediments from Odiel river (Southwest Spain). *Environ. Int.* 29, 69–77. doi: 10.1016/S0160-4120(02)00147-2

Schauser, I., Hupfer, M., and Brüggemann, R. (2004). Spiel - A model for phosphorus diagenesis and its application to lake restoration. *Ecol. Model.* 173, 389–407. doi: 10.1016/j.ecolmodel.2003.10.033

SEMADS (2001). *Secretaria de Meio Ambiente e Desenvolvimento Sustentável. Bacia da Baía de Sepetiba*. (Rio de Janeiro: A Secretaria), 79.

Sen Gupta, B. K., Turner, R. E., and Rabalais, N. N. (1996). Seasonal oxygen depletion in continental-shelf waters of Louisiana: Historical record of benthic foraminifers. *Geology* 24, 227–230. doi: 10.1130/0091-76131996024<0227:SODICS<2.3.CO,2

Silva, M. A. M., da, Schreiber, B. C., and Santos, C. L. (2000). Evaporitos como recursos minerais. *Rev. Bras. Geof.* 18, 338–350. doi: 10.1590/s0102-261x2000000300011

Silva, Y. J. A. B., Cantalice, J. R. B., Singh, V. P., Scimento, C. W. A., and Wilcox, B. P. (2019). Heavy metal concentration and ecological risk assessment of the suspended sediments of a multi-contamited Brazilian watershed Acta Scientiarum. *Agronomy* 41:e42620. doi: 10.4025/actasciagron.v41i1.42620

Souza, A. C. B., Esteves, M. C. B., Nascimento Junior, D. R., Lima, N. O., and Silva, A. R. C. (2017). Geoquímica inorgânica e orgânica dos folhelhos da Formação Pimenteiras: implicações para um sistema petrolífero não convencional. *Revista do Instituto de Geociências* USP 17, 44–60.

Souza, A. M., Rocha, D. S., Guerra, J. V., Cunha, B. A., Martins, M. V. A., and Geraldes, M. C. (2021). Metal concentrations in marine sediments of the Rio de Janeiro Coast (Brazil): a proposal to establish new acceptable levels of contamination. *Marin. Pollut. Bull.* 165:112113. doi: 10.1016/j.marpolbul.2021.112113

Stein, R. (1991). *Accumulation of organic carbon in marine sediments. Results from the DSDP/ODP*. (Berlin: Springer-Velarg), 217.

Sutherland, R. A. (2000). Bed sediment-associated trace metals in an urban stream, Oahu, Hawaii. *Environ. Geol.* 39, 611–627. doi: 10.1007/s002540050473

Swarnalatha, K., Letha, J., and Ayoob, S. (2013). Ecological risk assessment of a tropical lake system. *J. Urban Environ. Engin.* 7, 323–329. doi: 10.4090/juee.2013.v7n2.323329

Thomson, J., Nixon, S., Croudace, I. W., Pedersen, T. F., Brown, L., Cook, G. T., et al. (2001). Redox-sensitive element uptake in north-east Atlantic Ocean

sediments (Benthic Boundary Layer Experiment sites). *Earth Planet. Sci. Lett.* 184, 535–547. doi: 10.1016/s0012-821x(00)00347-2

TIBCO Software Inc (2018). *Statistica (data analysis software system), version 13*. Available online at: http://tibco.com (accessed March 18, 2020).

Turekian, K. K., and Wedepohl, K. H. (1961). Distribution of the Elements in Some Major Units of the Earth's Crust. *Geol. Soc. Am. Bull.* 72, 175–192. doi: 10.1130/0016-7606(1961)72[175:doteis]2.0.co;2

Urban, N. R., Ernst, K., and Bernasconi, S. (1999). Addition of sulfur to organic matter during early diagenesis of lake sediments. *Geochim. Cosmochim. Acta* 63, 837–853. doi: 10.1016/s0016-7037(98)00306-8

Van de Bund, W., and Solimini, A. (2007). *Ecological Quality Ratios for ecological quality assessment in inland and marine waters*. Luxembourg: Office for Official Publications of the European Communities.

Vilela, C. G., Batista, D. S., Batista-Neto, J. A., Crapez, M., and Mcallister, J. J. (2004). Benthic foraminifera distribution in high polluted sediments from Niterói Harbor (Guanabara Bay), Rio de Janeiro, Brazil. *Anais Da Acad. Brasileira de Ciências* 76, 161–171. doi: 10.1590/s0001-37652004000100014

Villena, H. H., Dias Pereira, S. D., Chaves, H. A. F., Dias, M. S., and Josefa Varela Guerra, J. V. (2012). "Indícios da variação do nível do mar na Baía de Sepetiba," in *Baía de Sepetiba: Estado da Arte*, eds M. A. C. Rodrigues, S. D. Pereira, and S. B. Santos (Rio de Janeiro: Editora Corbã, 2012)

Wang, H. F., Yang, J. P., Pang, X. L., Chen, F., Liang, X., and Jia, J. T. (2016). Late Quaternary stratigraphic structure and sedimentary evolution of Lubei plain. *Acta Sedimentol. Sin.* 34, 90–101.

Wang, Q., and Morse, J. W. (1996). Pyrite formation under conditions approximating those in anoxic sediments I. Pathway and morphology. *Marin. Chem.* 52, 99–121. doi: 10.1016/0304-4203(95)00082-8

Warhurst, A. (1999). *Mining and the Environment: Case Studies from the Americas Editor(s)*. Available online at: https://www.idrc.ca/en/book/mining-and-environment-case-studies-americas. e-ISBN 1552503038 (accessed March 18, 2020).

Wasserman, J. C., Figueiredo, A. M. G., Pellegatti, F., and Silva-Filho, E. V. (2001). Environmental composition of sediments cores from a mangrove environment using neutron activation analysis. *J. Geochem. Explor.* 72, 129–146. doi: 10.1016/S0375-6742(01)00158-3

White, M. G. (1974). *Tin resources of Brazil. Open-File Report 74-333*. Available online at: https://pubs.usgs.gov/of/1974/0333/report.pdf (accessed March 18, 2020).

Zaninetti, L., Brönnimann, P., Beurlen, G., and Moura, J. A. (1977). La Mangrove de Guaratiba et la Baie de Sepetiba, État de Rio de Janeiro, Brésil: Foraminifères et écologie. *Arch. des Sci.* 30, 161–178.

Zheng, X.-J., Chen, M., Wang, J.-F., Li, F.-G., Yan, Y., and Liu, Y.-C. (2020). Ecological risk assessment of heavy metals in the vicinity of tungsten mining areas, Southern Jiangxi Province, soil and sediment contamination. *Int. J.* 29, 665–679. doi: 10.1080/15320383.2020.1763912

Zheng, Y., Anderson, R. F., Van Geen, A., and Fleisher, M. Q. (2002). Remobilization of authigenic uranium in marine sediments by bioturbation. *Geochim. et Cosmochim. Acta* 66, 1759–1772. doi: 10.1016/s0016-7037(01)00886-9

Zheng, Y., Anderson, R. F., van Geen, A., and Kuwabara, J. (2000). Authigenic molybdenum formation in marine sediments: a link to pore water sulfide in the Santa Barbara Basin. *Geochim. et Cosmochim. Acta* 64, 4165–4178. doi: 10.1016/s0016-7037(00)00495-6

Zou, C., Mao, L., Tan, Z., Zhou, L., and Liu, L. (2021). Geochemistry of major and trace elements in sediments from the Lubei Plain, China: Constraints for paleoclimate, paleosalinity, and paleoredox environment. *J. Asian Earth Sci.* 6:100071. doi: 10.1016/j.jaesx.2021.100071

Conflict of Interest: The authors declare that the research was conducted in the absence of any commercial or financial relationships that could be construed as a potential conflict of interest.

Publisher's Note: All claims expressed in this article are solely those of the authors and do not necessarily represent those of their affiliated organizations, or those of the publisher, the editors and the reviewers. Any product that may be evaluated in this article, or claim that may be made by its manufacturer, is not guaranteed or endorsed by the publisher.

Citation: Silva LCd, Alves Martins MV, Figueira R, Frontalini F, Pereira E, Senez-Mello TM, Castelo WFL, Saibro MB, Francescangeli F, Mello e Sousa SH, Bergamaschi S, Antonioli L, Bouchet VMP, Terroso D and Rocha F (2022) Unraveling Anthropocene Paleoenvironmental Conditions Combining Sediment and Foraminiferal Data: Proof-of-Concept in the Sepetiba Bay (SE, Brazil). Front. Ecol. Evol. 10:852439. doi: 10.3389/fevo.2022.852439